36. DEPOSITION AND PROVENANCE OF MIOCENE INTRACLASTIC CHALKS, BLAKE-BAHAMA BASIN, WESTERN NORTH ATLANTIC[1]

D. M. Bliefnick, Gulf Exploration and Production Co., Houston, Texas
A. H. F. Robertson, Department of Geology, University of Edinburgh, West Mains Road, Edinburgh EH 9 3JW, United Kingdom
and
R. E. Sheridan, Department of Geology, University of Delaware, Newark, Delaware

ABSTRACT

The Miocene Great Abaco Member of the Blake Ridge Formation, cored at Sites 391 and 534 in the Blake-Bahama Basin, consists predominantly of redeposited deeper-water foraminifer–nannofossil chalk and minor shallow-water carbonate material, interbedded with radiolarian–diatom mudstone deposited below the calcite compensation depth. The mudstones comprise the background rain of pelagic sediments that may have been deposited and/or reworked by weak contour currents. The chalks, including the distinctive intraclastic chalks, and skeletal packstones were deposited by turbidity currents, and less so by debris flows. These gravity flows eroded and entrained large numbers of siliceous mud and clay intraclasts, as well as lithified chalk and limestone clasts, some of shallow-water origin.

Possible sources of the carbonates include the Blake Plateau to the west and the Bahama Banks to the south. The Blake Plateau and Bahamian slopes provided the deeper-water foraminifer–nannofossil chalks, and the Bahama platform supplied the shallow-water carbonate grains and cemented limestone. Sea-level changes together with tectonism along the Great Abaco Fracture Zone and faults in the northern Bahamas may have provided the triggering mechanism that set large volumes of mostly unconsolidated carbonate material into motion. A submarine fan system and associated channels extending from the northern Bahamas into the Blake-Bahama Basin funneled debris flows and turbidites over 300 km into the basin, and subsequent turbidites filled in and leveled the topography, creating the prominant seismic reflector M. If similar deposits existed earlier in the Paleogene, they have been eroded, leaving only the Great Abaco Member as evidence of the tectonic and sedimentologic conditions existing in the western North Atlantic during the Paleogene and Miocene.

INTRODUCTION

At DSDP Site 534 a total thickness of 165.5 m of lower to middle Miocene sediments of the Great Abaco Member of the Blake Ridge Formation (Jansa et al., 1979) were cored. This Member, composed of siliceous mudstones, nannofossil chalk, intraclastic chalks, and redeposited shallow-water limestones was also cored at Site 391, 22 km to the southwest, where it reaches 500 m in thickness (Benson, Sheridan, et al., 1978). Seismic mapping and piston coring (Sheridan et al., 1974) show that the Great Abaco Member has a thickness of about 500 m throughout the Blake-Bahama Basin, pinching out against more typical greenish gray hemipelagic muds of the Blake Ridge Formation to the east, the Bahama and Blake outer ridges to the north, and the Blake Plateau to the west (Fig. 1).

In this chapter, we discuss and interpret the sedimentology and provenance of these unusual early Miocene sediments, previously interpreted as debris-flow deposits (Jansa et al., 1979). We conclude that most of the carbonate was redeposited from the southern part of the Blake Plateau and the adjacent Little and Great Bahama Banks, transported through the Great Abaco and Bahamas submarine canyon systems, and deposited over the Blake-Bahama Basin by predominantly turbidity-current mechanisms. Contrary to earlier ideas, only a small volume of the carbonates are true debris-flow deposits or deposits derived from shallow-water source areas. The turbidity currents spread out beneath the calcite compensation depth (CCD) eroding and entraining numerous clasts of partly consolidated siliceous mudstones to produce the characteristic intraclastic chalk facies cored at Sites 534 and 391.

STRATIGRAPHY

The base of the Great Abaco Member at Site 534 was sampled in Core 18 where greenish claystones appear, typical of the Bermuda Rise Formation (Jansa et al., 1979). At Site 391, 500 m of the Member were spot-cored and subdivided into five subunits (2a–e) (Benson, Sheridan, et al., 1978). Based on drilling depth and lithologic types recovered, only the lower 165.5 m were cored at Site 534, and were correlated with Subunit 2e of Site 391 (Sheridan, Gradstein, et al., this volume.)

The portion of the Great Abaco Member cored at Site 534 (Subunit 2e of Site 391) was divided into four subunits, 2a–d. These finer divisions of Subunit 2e of Site 391 are shown in Figure 2. The lower deposits (Subunit 2d) consist of relatively uniform greenish gray chalk and intraclastic chalk (Cores 15–18), which are moderately cemented. Within this interval, the number of clasts and the overall grain size decrease upward. Proceeding upward (Subunit 2c), the succession becomes more heterogeneous; it is composed of alternating light-colored

[1] Sheridan, R. E., Gradstein, F. M., et al., *Init. Repts. DSDP*, 76: Washington (U.S. Govt. Printing Office).

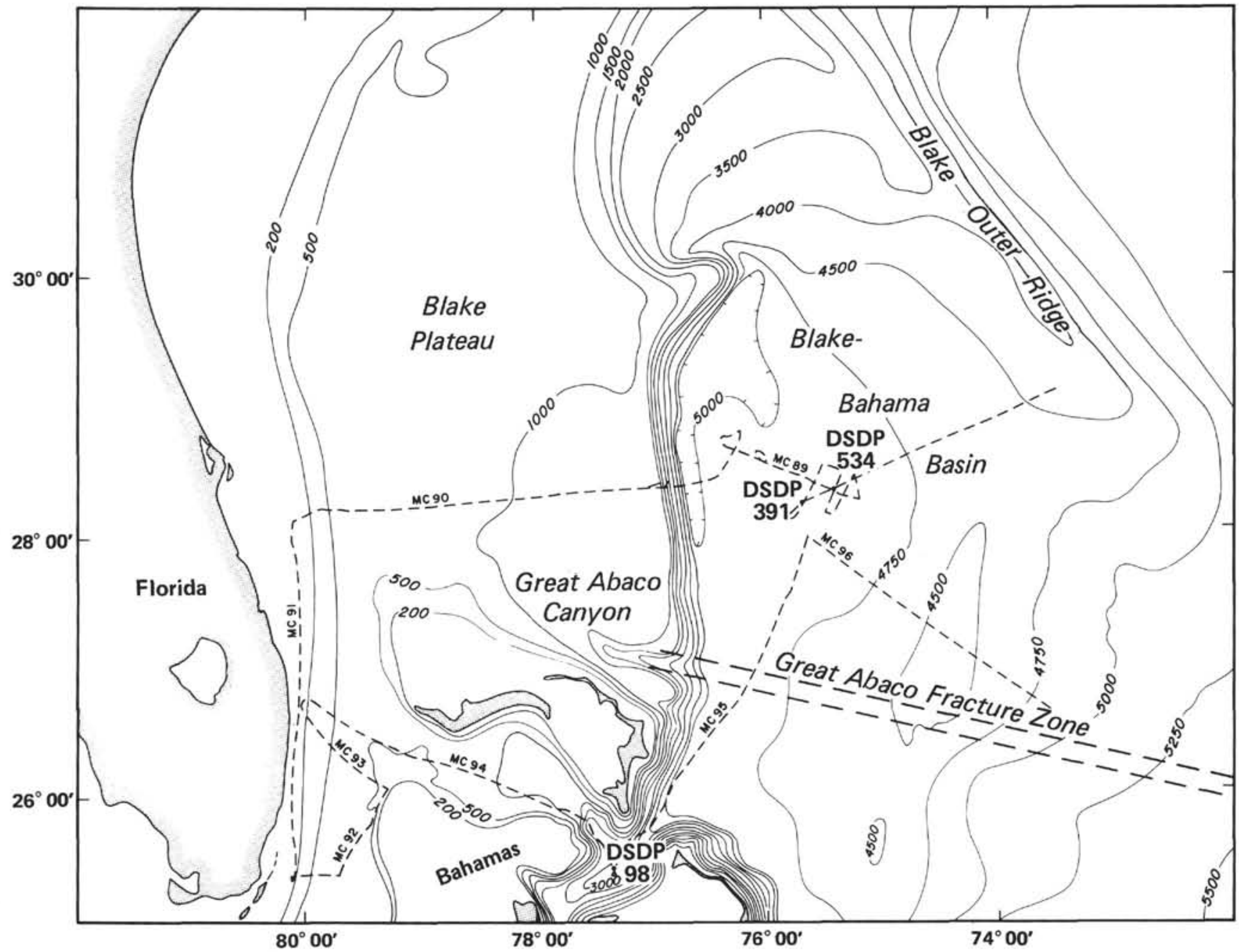

Figure 1. Bathymetric map showing the location of Sites 534 and 391 at which the Miocene Great Abaco Member of the Blake Ridge Formation was cored. (Location of the Great Abaco Canyon and Fracture Zone and seismic reflection profiles at Site 534 [dashed track line] are also shown [after Bryan et al., 1980]. Contours are in meters.)

chalks and olive gray mudstones, with minor volumes of intraclastic chalk, limestone clasts, impure porcellanite, and siliceous mudstone. In Subunit 2b, there is a repeated interval of intraclastic chalk, with one 4-m interval of siliceous mudstone near the top of the subunit and thinner intervals of calcareous mudstone lower in the subunit. The base of the chalk turbidite at the top of this subunit is a coarse bioclastic sand containing shallow-water benthic foraminifers. Subunit 2a, the shallowest sediment cored at Site 534, consists of alternations of siliceous mudstone and intraclastic chalk. The $CaCO_3$ (BOMB) data confirm that the redeposited carbonates are extremely calcareous, ranging up to 48% $CaCO_3$. By contrast, the siliceous mudstones mostly contain less than 10% $CaCO_3$.

LITHOFACIES

Within the cored Great Abaco Member at Site 534, the following lithofacies are recognized: (1) siliceous mudstone, (2) nannofossil chalk, (3) intraclastic nannofossil chalk, (4) skeletal packstone, and (5) pebbly chalk. Each of these lithologic types occurs in more than one stratigraphic subunit and is tied into a temporal framework in the Depositional Model section.

Siliceous Mudstone Facies

Lithology and Sedimentary Structures

Siliceous mudstones occur throughout the entire cored section, predominantly in Subunits 2a and c. The mudstones vary from massive to finely laminated to weakly or strongly burrow-mottled. Colors range from greenish gray to olive gray and bluish gray. Many intervals are structureless, apart from indistinct laminations and silty partings. Some intervals are highly to moderately burrowed, becoming slightly lighter colored upwards toward overlying redeposited chalk (Fig. 3A and B). Where the mudstone is burrowed it may be filled with paler-colored nannofossil chalk similar to the immediately overlying bed (Fig. 3B). Evidence of redeposition is seen in the small mudstone intraclasts (and rarely in chalk intraclasts) occasionally present in the mudstone. Laminations are rarely preserved as a result of extensive burrow mottling.

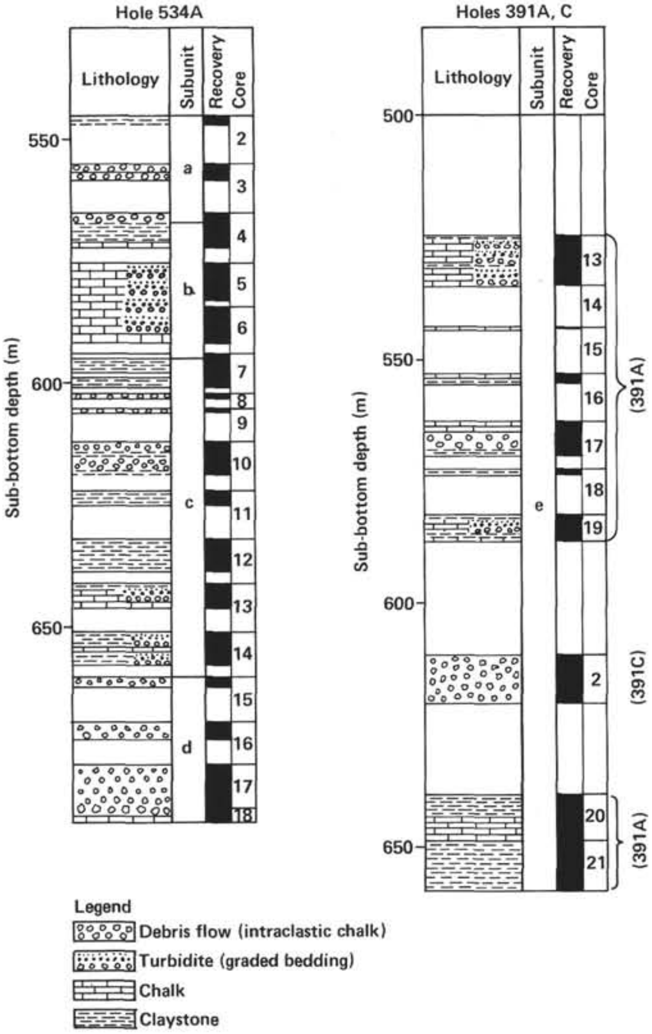

Figure 2. Generalized stratigraphic columns correlating the relative thickness, lithology, and core recovery of Sites 391 and 534 samples from the Miocene Great Abaco Member (after Sheridan, Gradstein, et al., this volume).

Petrography

The siliceous mudstone lithology could not readily be examined in thin section, but smear slides revealed the main constitutents. There is little petrographical variation throughout the Great Abaco Member, with most samples being composed of radiolarians, diatoms, lesser amounts of nannofossils, micritic carbonate, and terrigenous clays. No larger grains were observed except for intraclasts of the same composition, which made them difficult to distinguish petrographically. Preliminary studies by H. Chamley (personal communication, 1981) show that the siliceous mudstones consist of well crystallized smectite (60–90%), with palygorskite, sepiolite (up to 25%), plus some kaolinite and illite. There is little diagenetic alteration of matrix or grains and almost no precipitation of interparticle cement. Elongate radiolarians are oriented horizontally, and the clays further provide a laminated aspect to the samples.

Interpretation

The siliceous mudstones, containing radiolarians and diatoms and having low $CaCO_3$ values, are interpreted as "background" sediments deposited relatively slowly below the calcite compensation depth. The clay assemblage indicates a terrigenous detrital origin from an area with a warm climate and strong contrasts in humidity. This facies was probably deposited under conditions prevailing over much of the western North Atlantic during the Miocene. Nannofossils indicate deposition predominantly in the late early Miocene to early middle Miocene (Roth, this volume).

Sedimentary structures afford little or no evidence that any of the siliceous claystones were deposited by turbidity currents, like their counterparts further north on the Sohm, Hatteras, Nares, and Silver abyssal plains (data summarized in Jansa et al. 1979). On the other hand the sedimentary structures, including burrowing and indistinct planar laminations as well as bedding, are closely comparable with the middle to upper Pliocene sediments cored at Site 533 (Sheridan, Gradstein et al. this volume). These sediments are interpreted to be deposits of south-flowing contour currents believed to be responsible for sediment accumulations on the continental rise, and particularly, the Blake Outer Ridge (Hollister and Heezen, 1971). Thus the mudstones are not solely indigenous hemipelagic sediment but have in some cases undergone current redeposition.

Nannofossil Chalk Facies

Lithology and Sedimentary Structures

The nannofossil chalk facies occurs in every subunit, but is particularly abundant in Subunits 2b and c. The chalk is typically marly and yellowish gray, grading to greenish gray and light olive gray. Most of the nannofossil facies is massive or structureless. Contacts with the siliceous mudstone are sharp and distinct. In several cases, the chalk overlying the basal contact is well laminated and shows traces of grading. After deposition, the chalk was exposed on the seafloor and burrowed, especially in the upper portions (Fig. 4A and B). These relatively pure nannofossil chalks are frequently well cemented and transitional to limestone, in contrast to the intercalated siliceous mudstones and intraclastic chalks that are less indurated. In several cases, nannofossil chalk appears to grade upward into the volumetrically much more abundant intraclastic chalk.

Petrography

Nannofossils and planktonic foraminifers are the main constituents in this facies. The foraminifers (mainly globigerinids and globorotalids) tend to have open, unfilled tests near the top of the Member (Fig. 5A), whereas micrite or calcite spar tends to occlude the intraparticle porosity toward the base of the Member. Other grains include thin bivalve shells, sponge spicules, and recrystallized skeletal fragments. The matrix consists of fine pieces of these grains, as well as nannofossils (main-

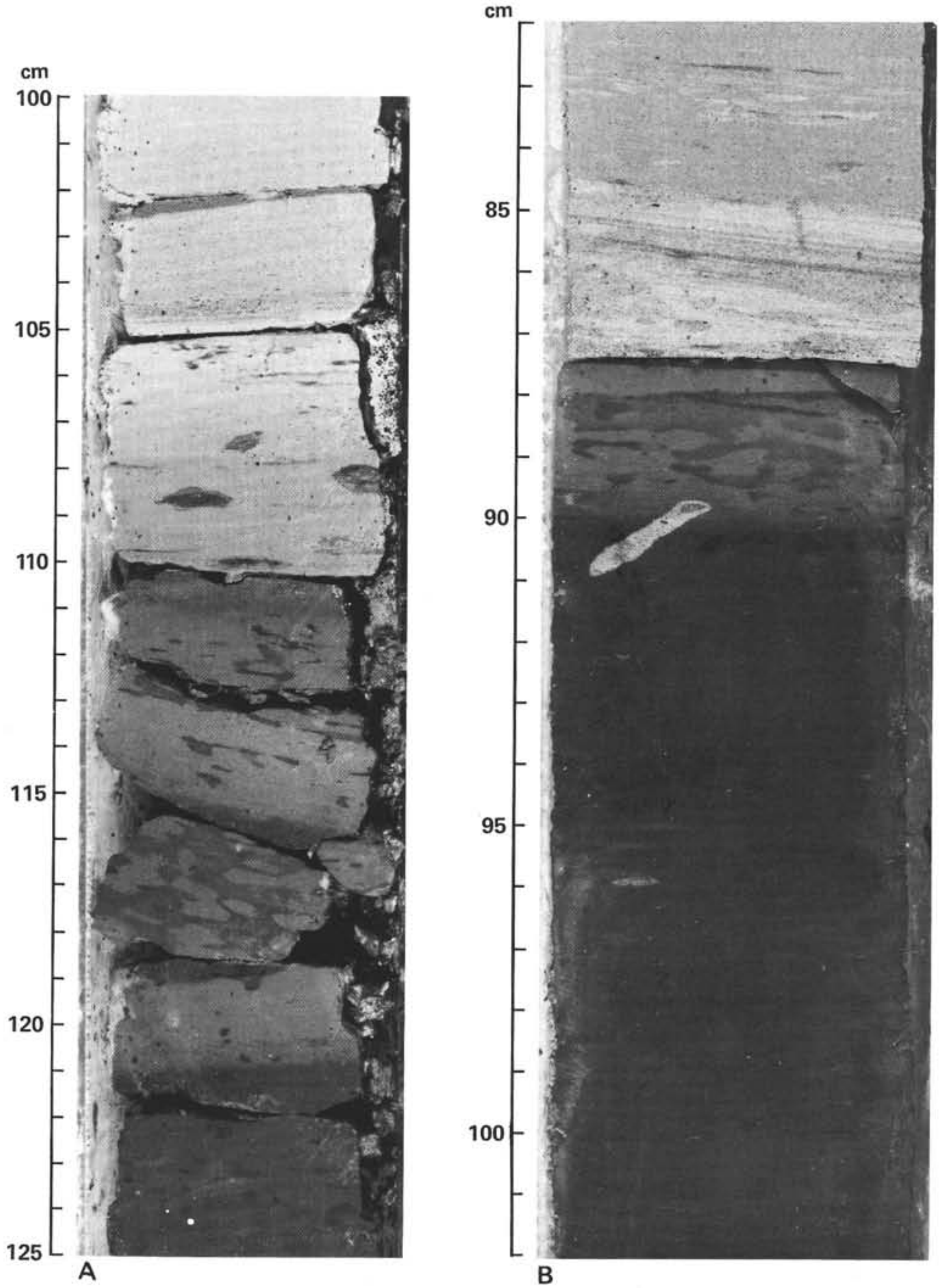

Figure 3. Siliceous mudstone facies. A. Siliceous mudstone below redeposited carbonate (111-112 cm in Sample 534A-5-2, 100-125 cm). (Note color variation and difference in burrow intensity. Burrows are horizontal and somewhat flattened. Primary current lamination is present only in the redeposited chalks, e.g., at 104 cm). B. Siliceous mudstone (88-100 cm in Sample 534A-4-2, 82-102 cm) overlain by calciturbidite. (Note absence of burrowing except beneath the turbidite and the 2-cm-thick pale interval [88-90 cm] cut by a carbonate-filled burrow. The color change dates deposition of the overlying turbidite. The chalk exhibits the scoured base, grading, cross- and plane-lamination typical of turbidite deposition.)

ly coccoliths, foraminifers, and discoasters), micritic carbonate, and rare dolomite rhombs (Fig. 5B). Textures are quite variable. Grainstones are more common toward the base of the formation where calcite spar has precipitated in many of the intra- and interparticle pore spaces. Elongate grains are unbroken and oriented parallel to bedding (Fig. 5C) and reflect the current activity and subsequent compaction during deposition of this facies. Where grains are abundant and occur close together, they are preferentially cemented by calcite and result in layers (Fig. 5D) that give rise to the laminated appearance observed in the cores.

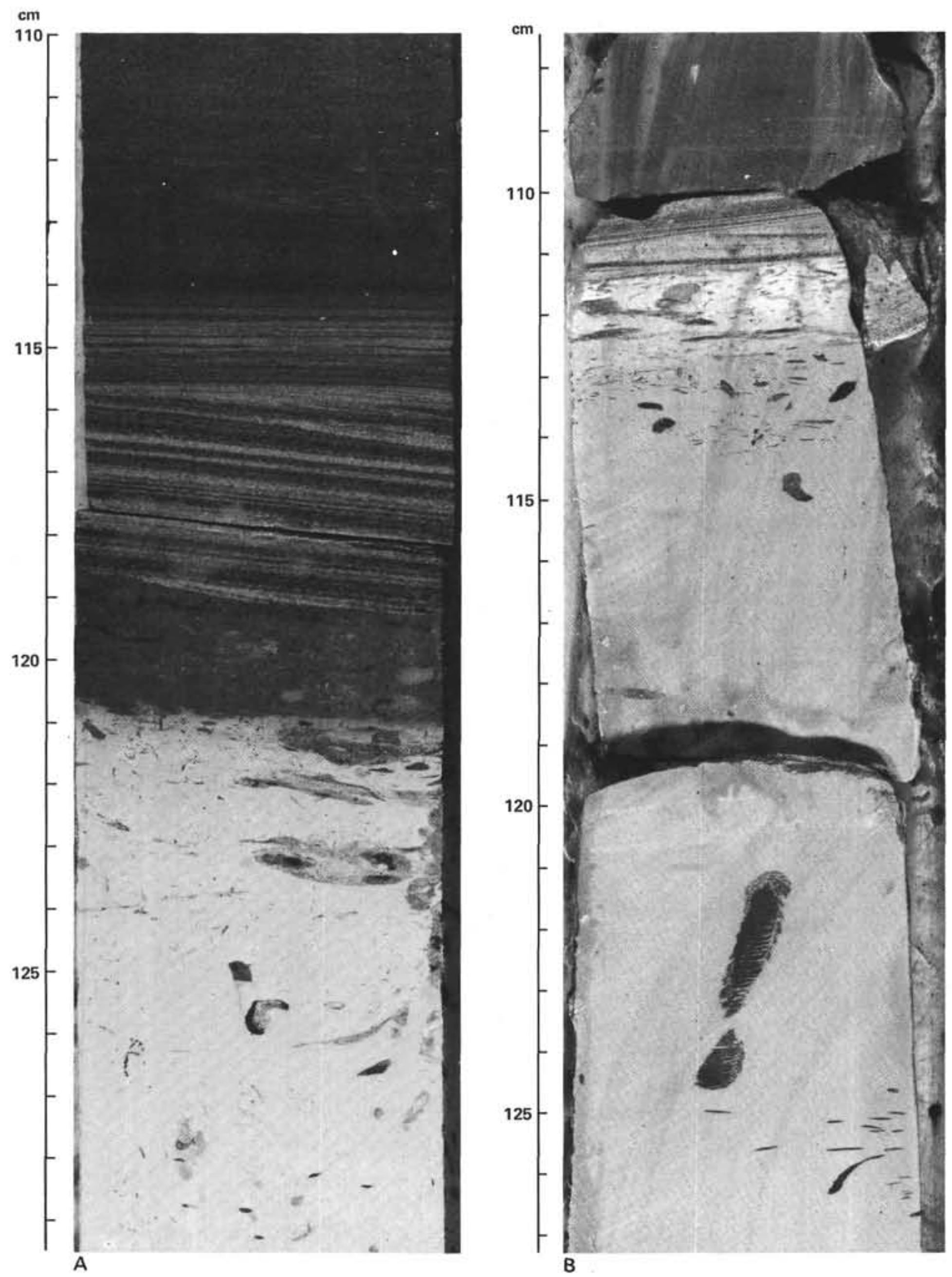

Figure 4. Nannofossil chalk facies. A. Nannofossil chalk (121–129 cm in Sample 534A-7-1, 110–129 cm) underlying redeposited limestone and siliceous mudstone. (Note irregular flattened burrows and absence of primary current lamination in the chalk. The scoured base and cross-lamination indicates the mixed limestone–mudstone was deposited by a turbidity current.) B. Nannofossil chalk (111–123 cm in Sample 534A-5-3, 108–126 cm). (Note calciturbidite base [110–111 cm] overlying homogenous nannofossil chalk, which is massive, apart from scattered burrows. Siliceous mudstone overlies the thin calciturbidite.)

Interpretation

The homogenous nannofossil chalk facies is redeposited into the background siliceous mudstone facies. The almost structureless (but showing some lamination and grading) foraminifer–nannofossil chalks were likely deposited from relatively gentle, dilute turbidity currents that were insufficiently powerful to erode and carry mudstone intraclasts. These calciturbidites consist entirely of slope-derived, redeposited pelagic material (dominated by coccoliths and planktonic foraminifers) without a terrigenous or shallow-water limestone component. The well preserved condition of the fossils indicates the turbidites were deposited so rapidly that they were preserved even though they were below the calcite compensation depth. As in the siliceous mudstones, nannofossils indicate deposition in the late early Miocene to early middle Miocene (Roth, this volume).

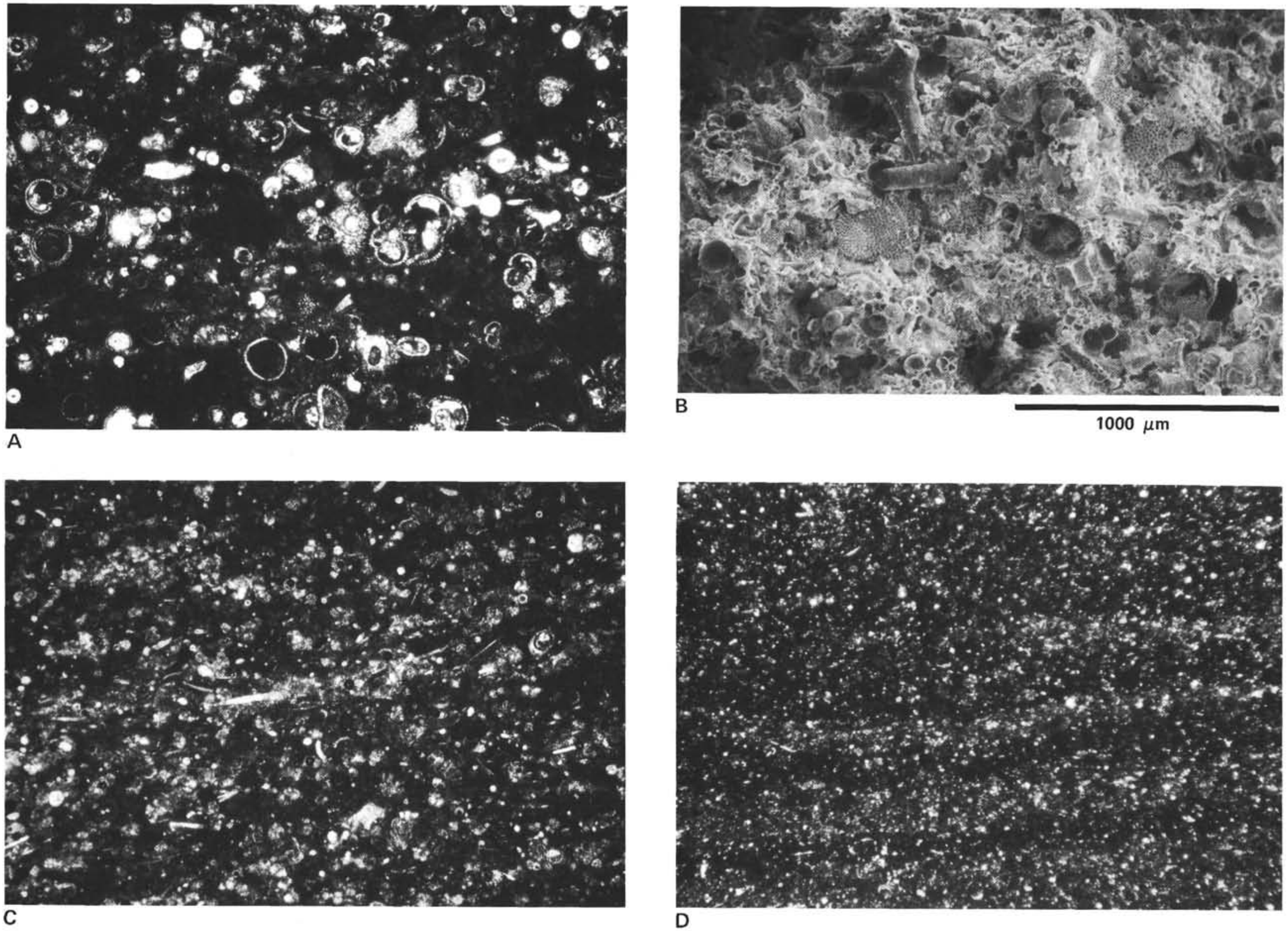

Figure 5. A. Sample 534A-3-2, 79–81 cm. (Thin-section photomicrograph of a planktonic foraminifer–nannofossil chalk with a packstone to grainstone texture. Intra- and interparticle porosity is high, and most of the black areas are open pore spaces. Width of field of view is about 5 mm.) B. Scanning electron micrograph of the same foraminifer–nannofossil chalk (Fig. 5A) showing the fine matrix components, the open, porous structure, and lack of cement. C. Sample 534A-5-1, 128–130 cm. (Thin-section photomicrograph of a sample of foraminifer–nannofossil chalk where elongate grains, especially sponge spicules, have been oriented parallel to bedding by gentle currents. Width of field of view is about 5 mm). D. Thin-section photomicrograph of the chalk sample in Fig. 5C showing preferentially cemented layers that result in fine laminations seen in cores. (Width of field of view is about 12 mm.)

Nannofossil chalk spot-cored at Site 391 includes a major 56-m-thick bed of remarkably uniform, white, clay- and silt-size carbonate, consisting of planktonic foraminifers and nannofossils (Site 391, Subunit 2a; Benson, Sheridan, et al., 1978). Although this major redeposited chalk lies well above the interval cored at Site 534, it indicates the similarity in lithologies and depositional processes between the two sites during this time.

Intraclastic Chalk Facies

Lithology and Sedimentary Structures

The Great Abaco Member at Site 534 is volumetrically dominated (especially Subunits a, b and d) by intraclastic chalk and minor intraclastic limestone. The matrix of these rock types is a chalk identical to that in the nannofossil chalk facies. The intraclasts are similar lithologically to the siliceous mudstone facies, varying in color from yellowish and greenish gray to greenish black and light bluish gray (Fig. 6C). Limestone intercalations are more extensively cemented with calcite, but otherwise are texturally similar to the chalk. These cemented intervals occur most frequently toward the base of the cored Great Abaco Member. In contrast to the siliceous mudstones, the intraclastic chalks have undergone little bioturbation. The laminations delineated by the horizontally oriented clasts are undisturbed (Fig. 6B) and indicate that rapid deposition of intraclastic chalk excluded the burrowing bottom fauna (Fig. 6A).

An unusually thick (about 25 m) intraclastic chalk horizon occurs in Cores 15, 16, and 17. The matrix is a marly, skeletal–nannofossil chalk-limestone with several types of claystone and limestone clasts. Within Core 17, grading in individual levels is subtle, but the limestone clasts are most abundant near the base of the intraclastic chalk and progressively decrease in size and number upward. This major intraclastic chalk unit appears to continue unbroken through Core 16 into Core 15, in which there was little recovery. Limestone clasts are still present in Core 16, and siliceous mudstone clasts like those of Core 17 are again abundant. The chalk in Core 15 is composed largely of homogeneous nannofossil chalk with few intraclasts. This major intraclastic chalk interval is then overlain by more heterogeneous chalks, calcarenites, and siliceous mudstones. Higher parts of the succession (e.g., Core 10) are again dominated by intraclastic chalks. The variation in the number of clasts and the shades of matrix color imply that individual intraclastic chalks are, in detail, amalgamated. Such contrasts may also be picked out by increased abundances of unusually large mudstone clasts.

Petrography

The intraclastic chalk is similar to the nannofossil chalk in that the main constituents are planktonic foraminifers and nannofossils (Fig. 7A). The redeposited nature of the facies is highlighted by the other grains, which include sponge spicules, fragments of benthic foraminifers and echinoderms, chalk, limestone and siliceous mudstone clasts, thin-shelled bivalves, rare grains of glauconite, phosphate, pyrite, and dolomite, occasional grains of red algae, and pieces of calcite that are unidentified skeletal fragments (Fig. 7B, C). The matrix is composed of nannofossils, carbonate mud, clay, and comminuted bits of skeletal debris (Fig. 7D). This facies shows the same pattern of cementation as do the nannofossil chalks. Foraminifer tests tend to be open in shallow samples, porosity is high (10–25%, both intra- and interparticle), and there is little cement. Deeper samples show a reduced porosity (5–10%), foraminifer tests are filled with micrite or calcite spar (frequently geopetally), and there is more cement precipitated around grains (especially foraminifers and echinoderms). Textures are wackestones and packstones, and nonintraclast grains are usually close together or in contact.

The most noticeable and distinguishing feature about this facies, for which it is named, is the presence of siliceous mudstone intraclasts and, to a lesser extent, limestone intraclasts in the chalk matrix (Fig. 7C). These clasts, and other elongate grains as well, are oriented parallel to bedding, may even be imbricated, and are normally graded. Occasionally matrix and small grains may be deformed around the larger clasts. The intraclastic chalk may overlie nannofossil chalk (Fig. 7E) or siliceous mudstone (Fig. 7F) and invariably has a planar base. Parallel-laminated packstone frequently overlies the planar bases.

Interpretation

Intraclastic chalk, volumetrically the most abundant sediment type in the Great Abaco Member at Site 534, consists entirely of redeposited material. Whereas the siliceous mudstone intraclasts may have been locally derived from within the basin, both the nannofossil chalk and limestone were derived from above the carbonate compensation depth, most likely from the surrounding continental shelf and slope. In addition to Miocene nannofossils, these chalks also contain poorly preserved reworked coccoliths often of the Paleogene and Late Cretaceous (Roth, this volume). At Site 391, comparable intraclastic chalk was cored (Subunits 2b and 2d), and its deposition was attributed to debris flows.

Physical characteristics are similar. At both sites, the intraclastic chalk consists of clasts that are widely dispersed through a matrix of planktonic foraminifer–nannofossil chalk and marl; these intraclasts are very rarely in contact. The typical indistinct plane lamination and parallel orientation of clasts appear to be primary, and not due to flattening by overburden. In thick intraclastic chalk intervals, as in Cores 16 and 17 of Site 534, there is normal-size grading and decrease in abundance of clasts upward throughout the interval. Jansa et al. (1979) note that sedimentary structures in the intraclastic chalks of Site 391 include a few "cut-and-fill" surfaces, low-angle inclined lamination, graded intervals, and rare burrowing. Our examination of these cores indicates that many of the intraclastic chalks are also parallel bedded, with laminae often picked out by small angular mudstone clasts (e.g., Hole 391A, Core 5, Section 6). The sharp bases, grading, lamination, and other sedimentary structures indicate these chalks are not debris flows but are calciturbidites formed on a scale from several centimeters to several tens of meters in thickness. However, the sedimentary characteristics of these two types of depos-

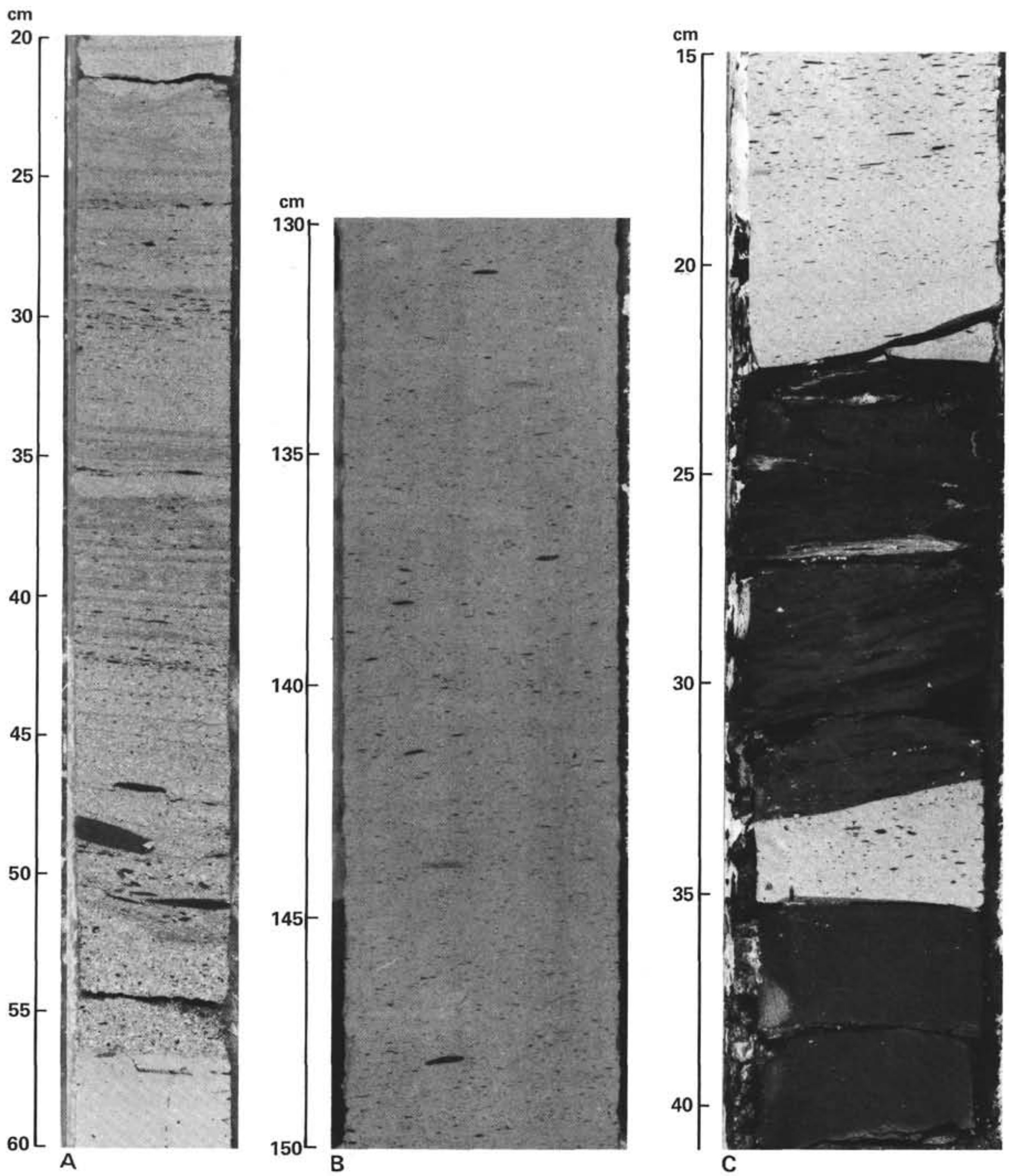

Figure 6. Intraclastic nannofossil chalk facies. A. Typical intraclastic chalk with sharp, scoured base above nannofossil chalk (57 cm in Sample 534A-4-2, 20–60 cm). (The graded base passes into a parallel laminated interval with siliceous mudstone intraclasts. The clasts decrease in size upward until the laminations can no longer be distinguished [20 cm].) B. Typical intraclastic chalk (Sample 534A-3-1, 130–150 cm). (Note the vague parallel fabric picked out by small elongate siliceous mudstone intraclasts in an otherwise massive chalk. The clasts were picked up as the chalk turbidite flowed over the background siliceous mudstone facies that covers the Basin.) C. Intraclastic chalk intercalated with (23–32 cm) and underlain by siliceous mudstone (35–41 cm) in Sample 534A-10-2, 15–41 cm. (The distorted character of the mudstone [23–32 cm] may have been caused by deposition of the chalk turbidites. This material is identical to the siliceous mudstone clasts within the chalk.)

its may be similar and may even grade into one another (Middleton and Hampton, 1973), as they do in Core 13 at Site 534. Debris flows usually show more inverse grading, a more chaotic arrangement of clasts, and a muddier matrix (Shanmugam and Benedict, 1978) than are seen in this facies.

Skeletal Packstone Facies

Lithology and Sedimentary Structures

Calcarenites composed of skeletal packstones make up a small percentage of the Great Abaco Member at Site 534, particularly in Subunit 2b. The calcarenites

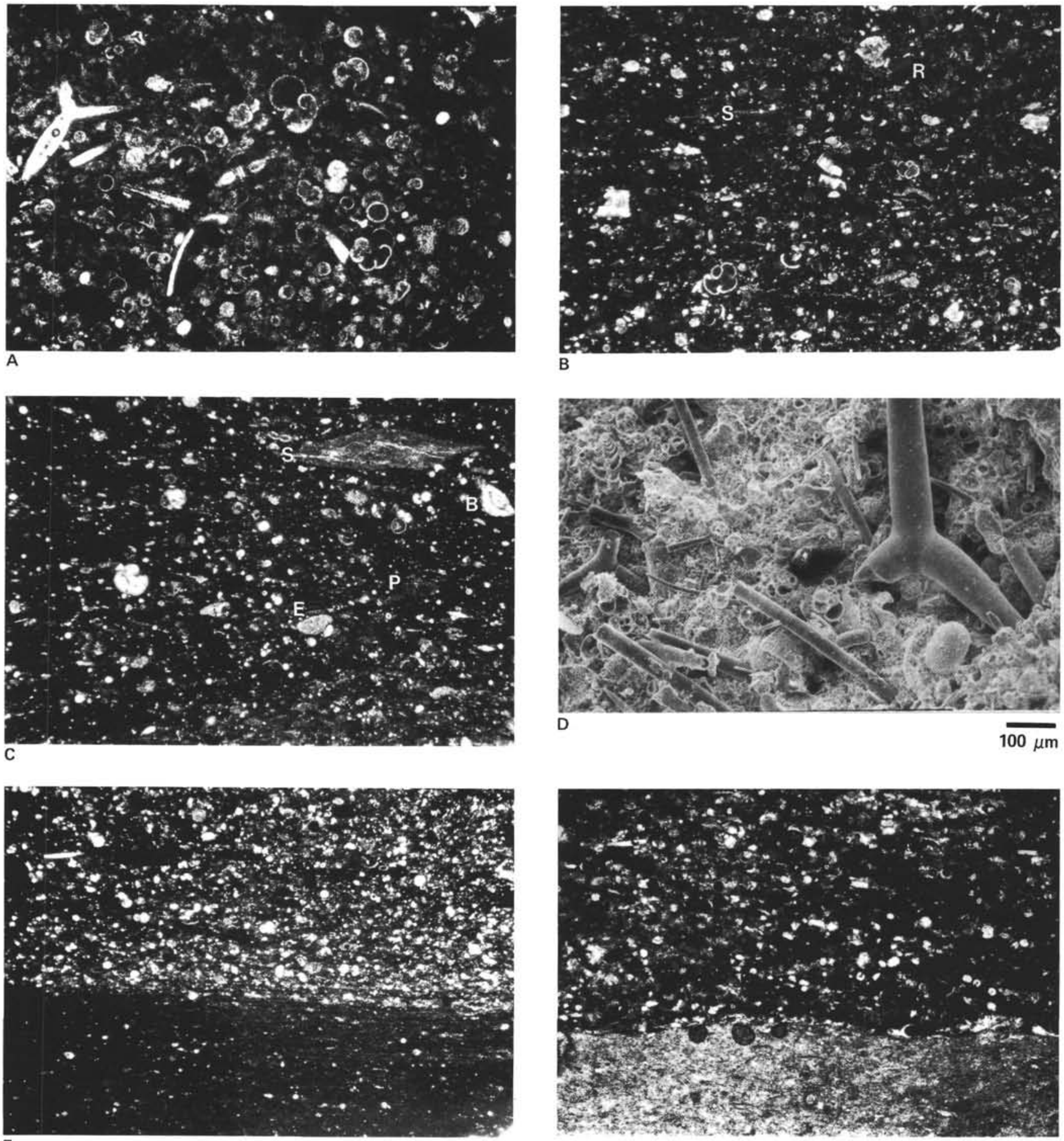

Figure 7. A. Sample 534A-10-4, 45–47 cm. (Thin-section photomicrograph of the intraclastic chalk facies. Prominent constituents include planktonic foraminifers and sponge spicules [including some triaxon spicules]. Foraminifer tests are mostly filled with matrix [a nannofossil micrite], and porosity is fairly low. Field of view is about 5 mm.) B. Sample 534A-17-4, 79–81 cm. (Thin-section photomicrograph of intraclastic chalk turbidite containing planktonic foraminifers, fragments of benthic foraminifers, red algae [R], siliceous mudstone clasts [S], and other skeletal debris in a micrite matrix. Field of view is about 12 mm.) C. Sample 534A-13-1, 93–95 cm. (Thin-section photomicrograph of intraclastic chalk turbidite containing planktonic foraminifers, benthic foraminifers [B], siliceous mudstone clast [S], echinoderm fragments [E] and phosphatic grains [P] in a micrite matrix. Note the horizontal orientation of elongate grains. Field of view is 12 mm.) D. Sample 391A-17-4, 67–70 cm. (Scanning electron micrograph of the intraclastic chalk matrix. The main constituents include nannofossil debris, small planktonic foraminifers, sponge spicules, and microcrystalline carbonate. Even at this level, the preferred orientation of elongate grains can be observed.) E. Sample 534A-4-5, 3–5 cm. (Thin-section photomicrograph of a laminated marly nannofossil chalk overlain by an intraclastic chalk composed predominately of planktonic foraminifers. The sharp, planar contact indicates deposition was probably from a turbidity current. Field of view is 12 mm.) F. Sample 534A-11-1, 81–84 cm. (Similar to Fig. 7E, except the intraclastic chalk is overlying a silicified zeolitic clay. Field of view is 5 mm.)

typically range up to 30 cm in thickness, are frequently in scoured contact with underlying nannofossil chalk or siliceous mudstone, and may exhibit grading, parallel lamination, and cross-lamination (Fig. 8A and B). The color is typically yellowish gray with some bioturbation towards the top. Often the graded units are quite thin and amalgamated, but occasionally a single graded unit may be several tens of centimeters thick (Fig. 8B). These graded, parallel and cross-laminated calcarenites frequently contain prominent benthic foraminifers, including *Nummulites* and *Lepidocyclina*.

Petrography

The skeletal packstones have a nannofossil-rich micrite matrix and many other components similar to the chalk facies discussed earlier. What distinguishes this facies is the abundance of relatively large grains, of both pelagic and shallow-water origin, and the persistant packstone fabric. Grain types include planktonic foraminifers (mainly globigerinids), sponge spicules, large benthic foraminifers (including *Lepidocyclina* and *Amphistegina*), red algae (*Archaeolithothamnium*), rare

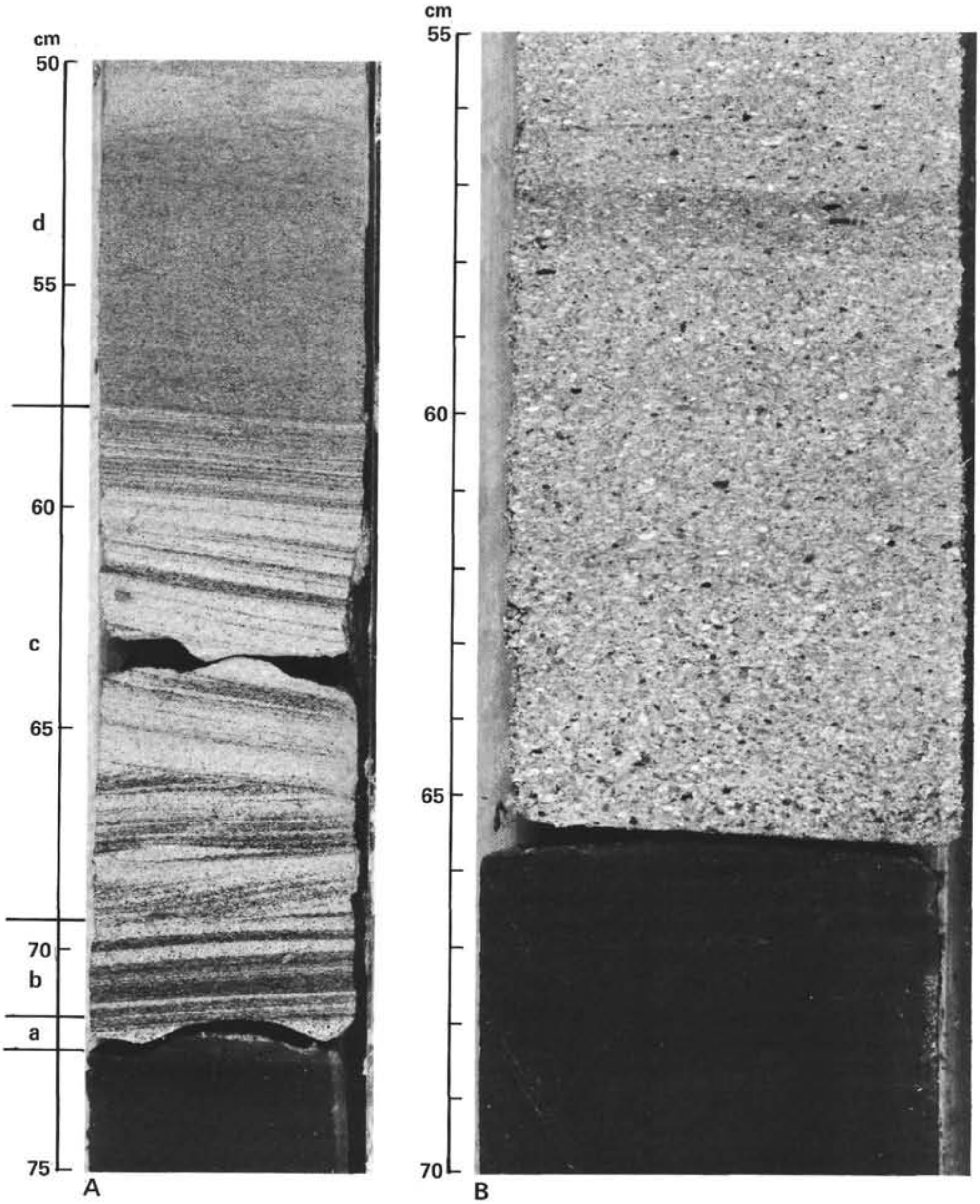

Figure 8. Skeletal packstone facies. A. Calciturbidite rich in skeletal fragments overlying siliceous mudstone (Sample 534A-12-2, 50–75 cm). (The scoured base, grading, parallel and cross-lamination probably represent Bouma a, b, c, and d divisions. Dark particles are minute intraclasts of siliceous mudstone.) B. Base of calciturbidite overlying siliceous mudstone (Sample 534A-7-1, 55–70 cm). (Sharp base, grading, and parallel laminations are probably Bouma a and b divisions. This packstone contains benthic foraminifers and other shallow-water constituents, indicating a shelfal source for much of this turbidite.)

green algae, echinoderm fragments, thick-shelled bivalves, cryptocrystalline grains, clasts of chalk containing planktonic foraminifers and sponge spicules, siliceous mudstone clasts, pelletal clasts, scattered pyrite, dolomite, glauconite and phosphate, and unidentified skeletal debris (Fig. 9A and B). Although the shallow-water components comprise only a small percentage of the total grains, they are important in the interpretation of the facies. This facies tends to be porous with only a small amount of cementation around grains (e.g., syntaxial overgrowths on echinoderms) and in the matrix. Porosities range from 10 to 20% in shallow samples but may be as low as 5% near the base, where more cement has precipitated (Fig. 9C). The amount of cement present may be attributed to the presence of shallow-water grains of unstable mineralogy that dissolve fairly quickly and reprecipitate as cement. Elongate grains are oriented horizontally and all grains are closely packed and in contact. Above planar to scalloped and clearly erosional bases (Fig. 9D), individual packstone units grade upward to finer sizes and better sorting.

Interpretation

The graded packstones are interpreted as calciturbidites derived from mixed shallow-water and deep-water sources. The a–d, b–d and d–e intervals as documented in clastic turbidites (Bouma, 1962) are present. The shallow-water, redeposited material is concentrated in the basal layers, relative to the finer-grained nannoplankton that remained in suspension longer and were deposited higher in individual turbidites. Siliceous mudstone intraclasts are also restricted to basal portions and are often concentrated in laminations. Upon entering the Basin, the turbidites pick up siliceous mudstone clasts that mix with the shallow-water components, but tend to disappear upward as the turbidite wanes. The lithology may then change into parallel and sometimes convolute-laminated or massive nannofossil chalk or back into siliceous mudstone (Fig. 8A). Most of the planktonic foraminifers are Miocene, but the coccoliths and benthic foraminifers are frequently reworked from Eocene or Upper Cretaceous strata (Moullade and Roth, in Sheridan, Gradstein et al., this volume). Similar graded calcarenites were recognized by Benson, Sheridan, et al. (1978) at Site 391, especially in Subunit 2e. Some samples are coarse enough to be calcirudites. Like those at Site 534, these calciturbidites were derived from both pelagic and shallow-water sources, and contain planktonic and benthic foraminifers, red algae, echinoderms, mollusks, ostracodes, and peloids.

Pebbly Chalk Facies

Lithology and Sedimentary Structures

Although the debris-flow deposits are volumetrically minor, they constitute an important facies and occur at several horizons at Site 534, especially in Subunit c. Individual debris-flow intervals exhibit sharp, though not usually erosional, bases. The debris material, which includes siliceous mudstone, nannofossil chalk, and some limestone, frequently occurs as intervals of convolute laminated and folded siliceous mudstone and indurated chalk (Fig. 10B). Highly deformed siliceous mudstone clasts are up to 4 to 5 cm long, much larger than in the typical intraclastic chalk. Local inverse grading occurs on a scale of several tens of centimeters. Intraclasts include limestone, which contains shallow-water benthic foraminifers, indicating a partial shallow-water source for the debris flow. Debris flows were not cored elsewhere except for several centimeters at the base of a graded calciturbidite in Core 6 (Fig. 10A), and possibly at the base of a skeletal packstone turbidite in Core 17, Section 6.

Debris-flow deposits were also cored at Site 391 (Fig. 11). The debris flows had a variety of sources from shallow shelf to deeper slope, and clasts include siliceous mudstone, chalk, and limestone. Like those at Site 534, the clasts float chaotically in and are supported by the predominantly chalk matrix. The debris-flow material exhibits convolute lamination and is frequently interbedded with nannofossil chalk turbidites.

Petrography

The debris flows are very similar in appearance to some of the skeletal packstones. The matrix is a nannofossil-rich micrite that is moderately porous (5–10%) and has been fairly well cemented. There is a wide variety of clast type, including siliceous mudstone, nannofossil and intraclastic chalk, and shallow-water limestone. The limestone contains red algae, large benthic foraminifers, thick-shelled mollusks, miliolids, and rare coral. The clasts are coarse (several mm to 1 cm in diameter), rounded to angular, poorly sorted, and may be oriented parallel to bedding but more often exhibit a random or chaotic fabric (there is no consistent geopetal orientation from clast to clast). Unlike the skeletal packstones, the "grains" in this rock type are not in contact but are suspended in and supported by the matrix. On a fine scale, the matrix, grain, and clast composition is similar to that of the skeletal packstones. Only in looking at the larger-scale features are differences noted and characteristics typifying debris flows observed.

Interpretation

In contrast to the intraclastic chalks, the one major horizon of debris material at Site 534 was deposited by a true mass-flow mechanism. The criteria for recognizing debris flows have been described by several authors and include abundant muddy matrix, planar to undulating basal contact, random to parallel orientation of clasts, wide variety of clast types and sizes, occasional inverse grading, lack of evidence for turbulent flow, and floating or suspension of grains and clasts in the muddy matrix (Middleton and Hampton, 1973; Fisher, 1971; Walker 1979; McIlreath and James, 1979; Mountjoy et al., 1972; Enos, 1977; Shanmugam and Benedict, 1978). The deposits interpreted as debris flows at Site 534 exhibit many of these characteristics.

Clasts were derived from within the basin as well as from different parts of the adjacent carbonate platform. Shallow-water and slope carbonates are typically lithified very early, with lithified and unlithified layers

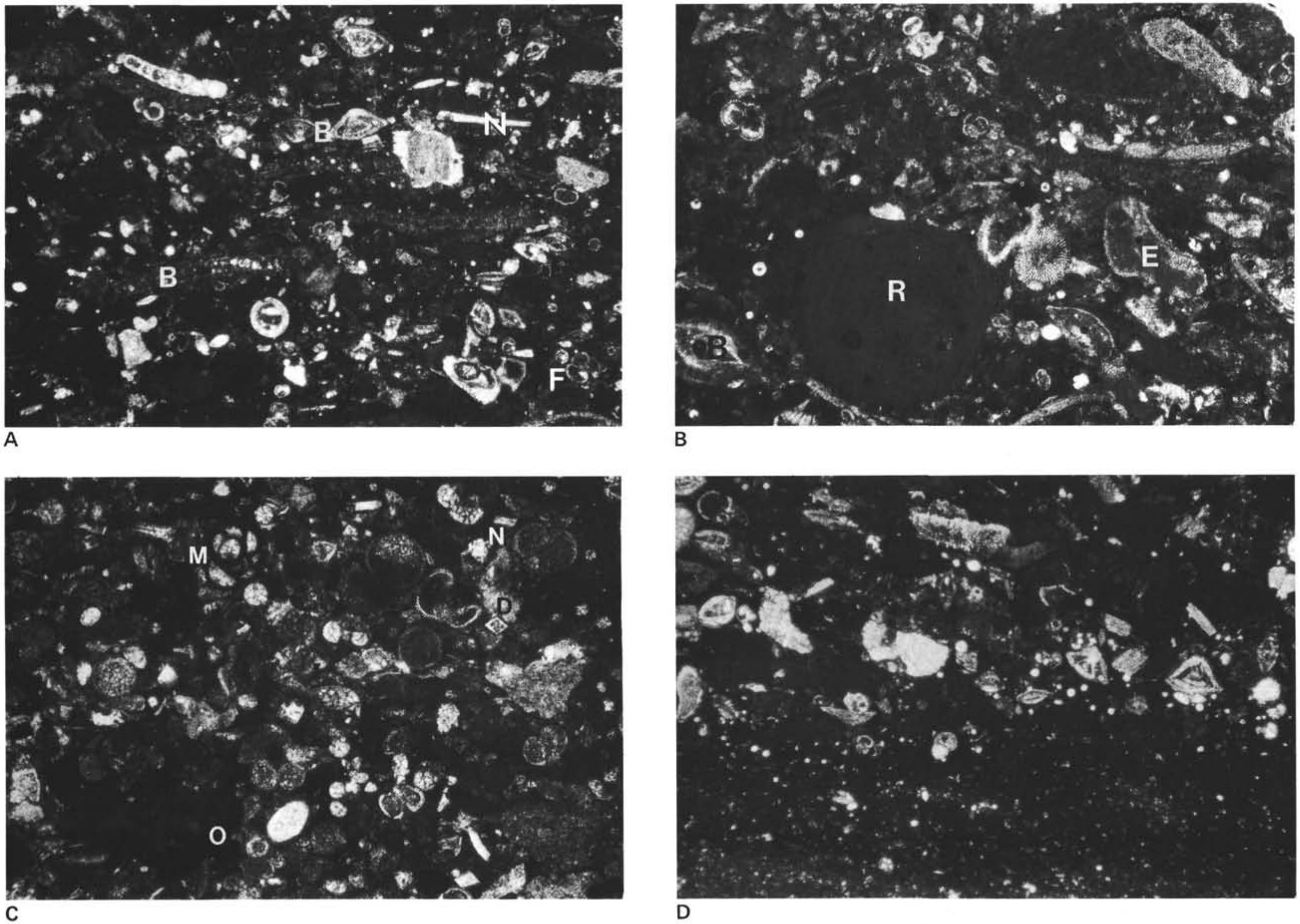

Figure 9. A. Sample 534A-7-1, 58–60 cm. (Thin-section photomicrograph of a skeletal packstone with both pelagic and shallow-water grain types. N = sponge spicules, B = benthic foraminifers, F = planktonic foraminifers. Field of view is 12 mm.) B. Sample 534A-7-1, 58–60 cm. (Thin-section photomicrograph of a calciturbidite with prominent *Archaeolithoporella* [R], echinoderm plates [E], and benthic foraminifers [B]. Field of view is 5 mm.) C. Sample 534A-17-6, 131–133 cm. (Thin-section photomicrograph of skeletal packstone turbidite dominated by planktonic foraminifers. Other grain types include sponge spicules [N], a miliolid foraminifer [M], pyrite [O], and dolomite [D]. Planktonic foraminifer tests are geopetally filled with micrite and calcite-spar cement. Field of view is 5 mm.) D. Sample 534A-4-2, 57–59 cm. (Thin-section photomicrograph of a mixed-source calciturbidite overlying a planktonic foraminifer–nannofossil chalk. The contact is planar to scalloped and indicates erosion of the chalk by the turbidite. Field of view is 12 mm.)

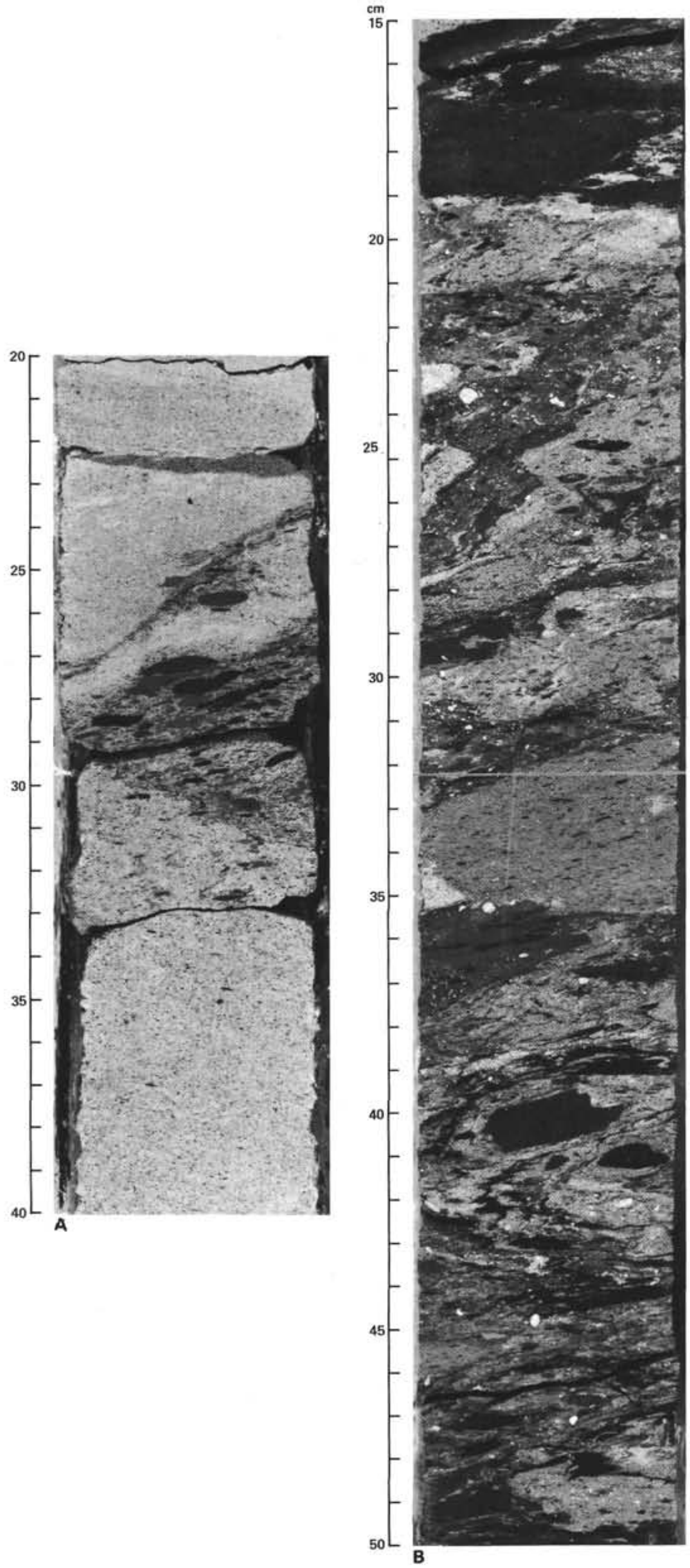

Figure 10. Pebbly chalk facies. A. Concentrated mass of siliceous mudstone intraclasts, of different colors and plasticity, within intraclastic chalk (Sample 534A-6-4, 20–40 cm). (These clasts are probably a localized mass flow entrained within the intraclastic chalk, which is a calciturbidite. B. A debris-flow interval with highly contorted siliceous mudstone and intraclastic chalk (Sample 534A-13-2, 15–50 cm). (The white grains are shallow-water limestone containing benthic foraminifers. This material is probably a portion of a debris flow that reached the Basin through Miocene submarine channels that extended to the northern Bahama Banks.)

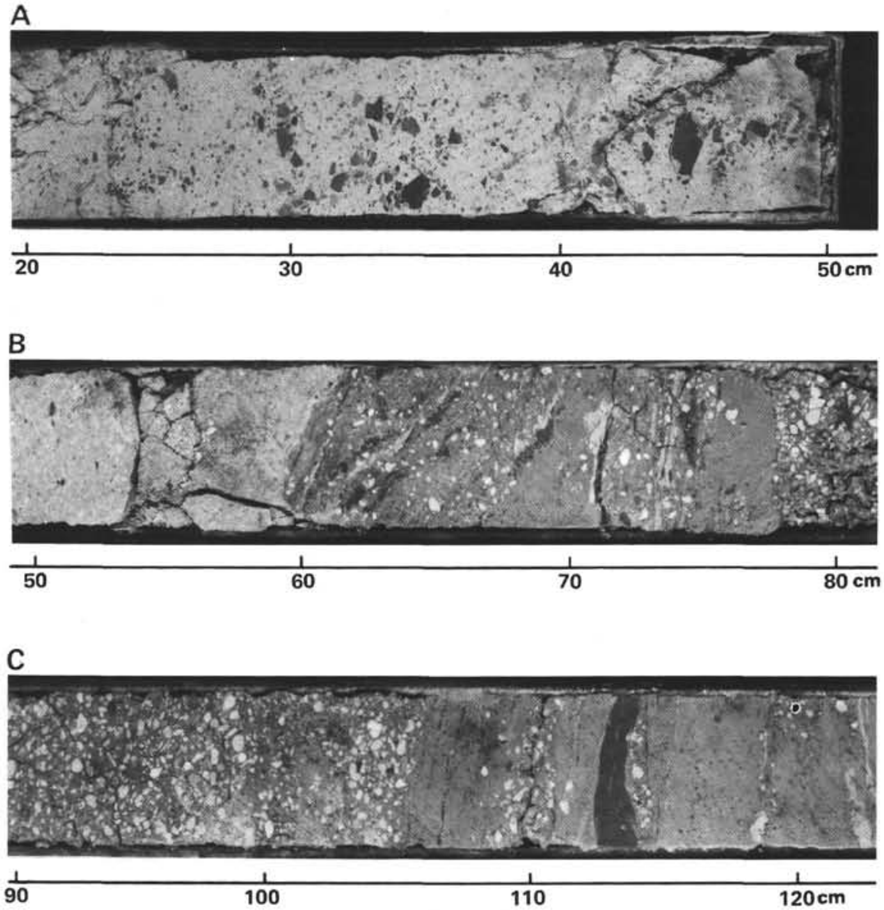

Figure 11. Pebbly chalk facies. A. An intraclastic chalk debris flow from Site 391 (Sample 391A-5-5, 20–50 cm). (The large angular clasts of dark siliceous mudstone, which were partially lithified prior to entrainment in the flow, float chaotically in the chalk matrix; overall, the rock is poorly sorted.) B and C. This intraclastic chalk debris flow from Site 391 (Sample 391A-12-5, 50–80 cm and 92–123 cm) contains subrounded clasts of white, shallow-water limestone. (The limestone was well cemented before being eroded and indicates a different source for the debris material than that in Fig. 8A.)

in part reflecting slow and rapid sedimentation (McIlreath and James 1979). Earthquakes, tsunamis, or simply overloading of sediment may trigger the release and surge of a slurry of cemented and uncemented shallow and mid-depth material, which picks up basinal contributions as it enters deep water. The fine intercalations of siliceous mudstone, intraclastic chalk, and limestone indicate mixing was extensive. Reported ancient submarine debris flows range from very large-size clasts (Mountjoy et al., 1972) to rather fine-grained deposits (Shanmugam and Benedict, 1978). Those at Site 534 would be considered fine-grained. After transport the high density and high viscosity of the slurry caused deposition to take place as a unit rather than gradually upward. This type of deposition explains the lack of traction and internal shearing features, the lack of normal grading and parallel lamination, the random to chaotic orientation of clasts, and the floating of clasts in the lime mud matrix (supported by the yield strength of the matrix). The fine-grained nature of the deposit may be a function of the source areas, but may also indicate that the strength of the flow was not sufficient to support larger clasts (Shanmugam and Benedict, 1978). The relatively minor amounts of debris-flow deposits probably reflect a combination of two factors: (1) the source area for the flows was distant, and flows did not often reach this far into the Basin, and (2) these periods of gravity-induced catastropic sedimentation were short, and the relatively quiet pelagic sedimentation of finer-grained turbidites predominated most of the time.

Notably, the debris-flow horizon at Site 534 occurs at the base of a major 10-m thick intraclastic chalk unit, which suggests the two could be a single event. Similar relationships exist in Cores 15, 16, and 17. Several authors have pointed out the close association of slumps, debris flows, turbidites, and contourites (Middleton and Hampton, 1973; Mountjoy et al., 1972; Shanmugam, 1980). A main point is whether enough water can be mixed into the slurry to create turbulent flow conditions. In subaqueous debris flows, Hampton (1972b) has shown that flow separation takes place on the upper part of the debris flow and that such separation is effective in mixing water into the flow and generating a turbulent cloud of less concentrated suspension, which then moves away as a turbidity current. Fine-grained debris flows and associated turbidites, such as those observed at Site 534, may be important as a major transporter of ocean sediments.

Benson, Sheridan, et al. (1978) interpreted that the major part of the Great Abaco Member cored at Site 391 had been deposited by gravity flows of a mud-flow or debris-flow type. We feel a much smaller volume of sediment was deposited due to these mechanisms. However, a continuous spectrum exists between the laminar flow of viscous slurries and turbulent flow of turbidites, and their deposits frequently occur together (Crevello and Schlager, 1980). Also, during different stages of flow, different mechanisms may dominate and sedimentary structures and textures will reflect these changes. The siliceous mudstone clasts in the intraclastic chalks are aligned and oriented horizontally, which, together with occasional grading, indicates turbulent flow. However, they are also isolated and floating in the matrix, which indicates a slurry dense and viscous enough to prevent the clasts from settling into a grain-on-grain structure. We envision a close relationship between fine-grained debris flows and fine-grained turbidites, with the sediments grading from one to the other and showing characteristics of both.

DIAGENESIS

The Great Abaco Member has not been buried very deeply; the most conspicuous diagenetic feature is different degrees of calcite cementation. Typically the siliceous mudstones are indurated but not well lithified. Compaction and a small amount of calcareous cement are the main agents of lithification. The nannofossil chalk and intraclastic chalk become better cemented downward and may be transitional to limestone. Several intervals of limestone were initially interpreted on board ship as parts of boulder-sized clasts associated with debris flows and turbidites. However, rare lamination in the limestone is parallel to bedding, and apart from the degree of cementation, the sediments above and below are identical. In this section a single pyrite nodule was also noted, indicating the presence of at least localized reducing conditions.

There are several kinds of cement in the chalks. An early generation of acicular cement (probably originally aragonite) may be preserved inside some shallow-water benthic foraminifer chambers. This cement is succeeded by, and is encased in, a later generation of calcite spar. The most common cement is within and immediately around planktonic foraminifer tests (Fig. 12A). The skeletal packstones and debris flows are fairly well cemented. These facies initially had high depositional porosities in which carbonate cement later precipitated. The carbonate for cement was probably released largely from dissolution of transported shallow-water carbonate material, which consists of metastable aragonite and high-magnesium calcite. Even so, most of the cement in these facies (as well as the chalks) is micritic, with only minor amounts of coarser, pore-filling calcite spar (Fig. 12 B). The micritic cement is sometimes difficult to distinguish from the mud and skeletal grains that compose the matrix. The coarser carbonate material is broken

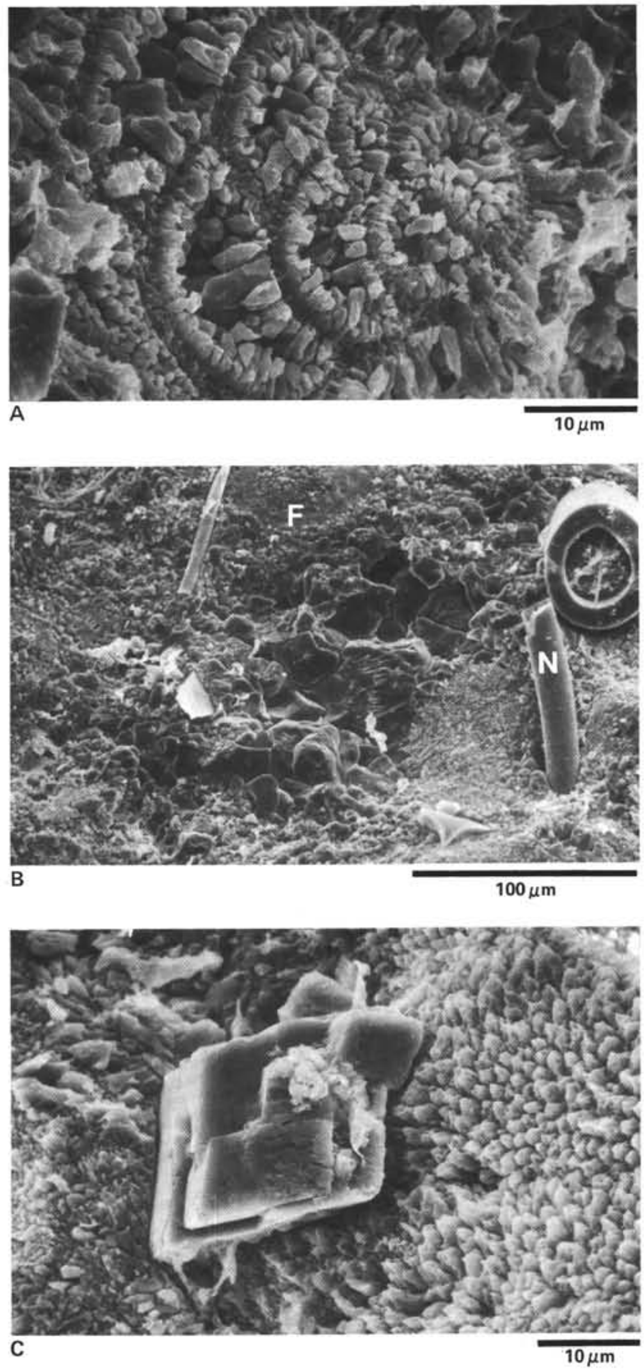

Figure 12. A. Sample 534A-5-5, 78–80 cm. (Scanning electron micrograph of a planktonic foraminifer with abundant intragranular calcite spar cement. The cement occludes most of the pore space within the test and extends for a short distance into the surrounding matrix.) B. Sample 534A-10-4, 45–47 cm. (Scanning electron micrograph of chalk matrix illustrating the predominantly micritic nature of the calcite cement, and one instance where the cement filled a pore and the crystals grew to microspar size. F = planktonic foraminifer tests. N = sponge spicule.) C. Sample 534A-17, CC. (Scanning electron micrograph of micritic-sized calcite cement and diagenetic dolomite rhomb, with two smaller rhombs extending at an angle from the surface.)

down during erosion, bioturbation, and cementation until it becomes a cryptic biogenic material that is virtually impossible even in SEM to classify or to distinguish from micritic cement. Dolomite rhombs are occasionally present in the skeletal packstone and debris-flow facies (Fig. 12C). They may be detrital dolomite transported from shallower regions or in-place diagenetic growth. With the shallow amount of burial, there has been some compaction but no pressure solution or development of stylolites.

PROVENANCE AND DEPOSITIONAL SETTING

The bulk of the carbonate at both Sites 391 and 534 was redeposited by a variety of sediment gravity flow mechanisms below the CCD where siliceous muds and clays were accumulating. In contrast to the suggestions of Benson, Sheridan, et al. (1978) and Jansa et al. (1979), only a small volume of material was deposited by debris-flow mechanisms *sensu strictu*. On board ship it was suggested that some inclined lamination in the nannofossil chalks and calcarenites was produced by bottom-current reworking. However, the associated cross-bedding to be expected in the indigenous siliceous mudstones is not seen; consequently, the inclined lamination is interpreted as a Bouma c interval of a calciturbidite. In addition, the sedimentary features of the siliceous mudstones are consistent with deposition from gentle, contour-flowing currents (Hollister and Heezen, 1971).

There are two candidates for provenance of the Great Abaco Member. The first, suggested earlier by Benson, Sheridan, et al. (1978) and Jansa et al. (1979), is the Bahama Banks area to the southwest, which obviously was a source of shallow-water carbonate material in the Miocene. The second possibility is the Blake Plateau to the west. Seismic mapping shows that the Great Abaco Member can be traced, by a series of closely spaced internal seismic reflectors, through most of the Blake-Bahama Basin (Jansa et al., 1979) up to the edges of both the Blake Plateau and the Bahama platform.

There are two possible sources for the material from the south: (1) the vicinity of Great Abaco Canyon situated between the south end of the Blake Plateau and Little Bahama Bank (Fig. 1), and (2) the area around Northeast Providence Channel (vicinity of DSDP Site 98 on Fig. 1). A possible modern analog for transport of this material into the Basin is the carbonate debris sheets and turbidites found in Exuma Sound (Crevello and Schlager, 1980). Exuma Sound is one of three intraplatform basins in Great Bahama Bank and forms a narrow elongate trough, which, at 2000 m, intersects an axial valley connecting the Sound with the Atlantic Abyssal Plain. In Exuma Sound, the Basin margin and interior consist of coarse clastic carbonates, which are shed episodically from the platform margins and slopes (Crevello and Schlager, 1980). These clastic carbonates are interbedded with hemipelagic carbonate muds and fines derived from the adjacent platforms. Up to 65% of the clastic carbonates deposited in the Basin were derived from shallow-water sources, with the remainder coming from the slope and the Basin itself. The main debris flow recognized by Crevello and Schlager was several tens of meters thick and covered the entire northwest half of the Basin as an unchannelized sheet flow, which then became channelized and confined to the axial valley in the southeastern portion of the Basin. The turbidite associated with the debris flow covered the whole Basin. Together they traveled over 160 km across the Basin and out onto the Atlantic Abyssal Plain. Several comparisons can be made between the Exuma Sound and Great Abaco debris-flow deposits. In terms of thickness, the largest debris-flow turbidite cored at Site 534 (Cores 15, 16, and 17) was also several tens of meters thick, and the flow that gave rise to it may have been much thicker. Source areas are similar, with contributions coming from shelf, slope, and basin, and interbedding of these different lithologies is seen in both locations. However, the Great Abaco contains a much smaller amount of shallow-water–derived redeposited carbonate, only about 10 to 15%. Because the amount of shallow-water carbonate material in the Great Abaco is less, the extent of platform margin failure required to produce the observed amount of sediment would be correspondingly less than that hypothesized by Crevello and Schlager (1980). Still, the event was unusual and sudden and was probably caused by a combination of catastrophic events such as hurricanes or tsunamis and local sediment overloading of the slope (Cook et al., 1972).

The second possible source for the Great Abaco member is the Blake Plateau and surrounding area. Knowledge of the subsurface geology of the Blake Plateau comes largely from Sites 390 and 392 of DSDP Leg 44 (Benson, Sheridan, et al., 1978), coupled with dredging and seismic studies (Ewing et al., 1966). The reconstructed cross-section of the Blake Nose cored at Sites 390 and 392 shows an irregular platform carbonate surface overlain by Early Cretaceous to Eocene pelagic chalks. The basal 48 m cored at Site 390 consist of oolitic limestone interbedded with chalky limestone thought to be shallow-water in origin. Well lithified shelf and lagoonal facies have also been dredged from the Blake Escarpment (Sheridan et al., 1971). Along the Blake Escarpment, all seismic reflectors are truncated obliquely by erosion. The middle Eocene is capped by a veneer of gravels and lag deposits indicative of strong bottom currents, which are known to sweep the area at the present time (Heezen et al., 1966). The history of post-Eocene deposition on the Blake Plateau is poorly known, also possibly due to current erosion. Piston coring on the Blake Plateau revealed Miocene *Globigerina* ooze and calcilutite, implying deep-water carbonate was being deposited and preserved at this time (JOIDES, 1965).

Seismic reflection studies of the Blake Plateau (Ewing et al., 1966) show that Great Abaco Canyon was already a major feature in the Late Cretaceous, was up to 700 m deep, and extended some 80 km northeast into the Blake Plateau as a broad elongate depression. Van Buren and Mullins (this volume) also note that the Canyon probably existed prior to the Campanian, based on a bathymetric depression in seismic reflector 4 in that area. The Great Abaco Canyon lines up with the Great Abaco Fracture Zone (Fig. 1), believed to date from the initial Atlantic opening and to have been rejuvenated in the Miocene (R. Sheridan, personal communication, 1981). The trend of this and other nearby fracture zones (e.g., Norfolk and Blake Spur fracture zones) is N 50 to 65° W and parallel to the major Atlantic Ocean fracture zones. Tectonic movements in the Tertiary involving the North and South American, and Caribbean plates may have rejuvenated the subparallel early Atlantic transform faults, including the Great Abaco Fracture Zone, as well as faults in the Northeast Providence Channel area (Fig. 13). Such fault activity could trigger movement of the surrounding sediment and generate sediment gravity flows. Sediment may have also been supplied from the northern margins of Little Bahama Bank where post-late Oligocene faulting and extensive slope instability have been documented (Mullins et al., in press; Mullins and Van Buren, in press; Van Buren and Mullins, this volume). The presence of Great Abaco Canyon for funneling the sediments also provides a plausible mechanism for getting the material into the Basin.

DEPOSITIONAL MODEL

The material in the Great Abaco Member was probably derived from both of the sources just discussed. The shallow-water material could not have come from the Blake Plateau, because a deep-water environment existed there during the Miocene. Most of the benthic and planktonic foraminifers in the Great Abaco Member are Miocene. However, several of the larger benthic foraminifers in the skeletal packstones and debris flows such as *Lepidocyclina* (common), *Nummulites* (few), *Assilina, Operculina*, and *Amphistegina* (rare), and *Discocylina* and *Heterostegina* (very rare) constitute a shallow marine assemblage from within the photic zone, tentatively assigned by Moullade (this volume) to the late Eocene. Thus these Eocene foraminifers could not have been derived from erosion along the Blake Escarpment or Great Abaco Canyon, because the youngest shallow-water material exposed there is Latest Cretaceous (Sheridan et al., 1971; Mullins et al., in press). However, much of the planktonic foraminifer–nannofossil chalk and intraclastic chalk could have come from the Blake Plateau area and flowed into the Blake-Bahama Basin via Great Abaco Canyon. Roth (this volume) notes that reworked Paleogene and Late Cretaceous coccoliths, eroded from older rocks exposed around the Basin, are numerous in the intraclastic chalk and other redeposited carbonates. We feel that a significant portion of the deeper-water chalks cored at Site 534 came from the Blake Plateau area. During the Miocene, the Great Abaco Fracture Zone, which controlled the location of the Great Abaco Canyon (Sheridan and Osborn, 1975; Benson, Sheridan, et al., 1978; Mullins et al., in press), was rejuvenated by Caribbean tectonic events. These tectonic events probably caused large volumes of consolidated and unconsolidated carbonate to slump repeatedly and slide into Great Abaco Canyon. There they became fluidized and spread out over the entire Blake-Bahama Basin as unconstrained, high-energy turbidity currents (Fig. 14).

The Bahama Banks are the logical source for the shallow-water material contained in the turbidites and debris flows cored at Site 534 (Fig. 14). They have been a shallow-water area since at least the Late Jurassic (Tator and Hatfield, 1975) and have supplied all the shallow-water fauna and flora from the Late Cretaceous to the Miocene. The deeper slopes of the Bahamian platform could also have supplied foraminifer–nannofossil chalks to the gravity flows, as in Exuma Sound (Crevello and Schlager, 1980). For example, the northern slope of Little Bahama Bank is dominated by calciturbidites and debris flows, but it is a thin sequence, which suggests that much of the material may have bypassed the slope, entered Great Abaco Canyon, and been transported into the Blake-Bahama Basin (Van Buren and Mullins, this volume). According to Van Buren and Mullins, the northern margin of Little Bahama Bank is a likely source for the displaced Miocene carbonates (Fig. 14) for several reasons: (1) during the Miocene it was the closest known carbonate shelf–slope environment, (2) Great Abaco Canyon existed in the Miocene and provided a ready conduit into the Blake-Bahama Basin for the shelf–slope derived sediment, and (3) slope instability and the generation of carbonate sediment gravity flows have persisted throughout the Cenozoic. Recurring changes in sea level, related to glacial peaks that are known to have occurred during the Miocene (Hayes et al., 1973), could have exposed broad areas of shallow sediments to cementation and erosion. Wave base would have moved up and down the platform margin paralleling sea level, causing sediment redistribution and additional instability (Crevello and Schlager, 1980). Fault activity added to this instability would provide the trigger mechanism for flow initiation. The same fault activity would also set deeper-water chalks into motion, and we feel that a significant portion of the chalks did come from the slopes of the Bahamian platform.

It would appear that the debris flows, being relatively coarse, would need some help to travel the more than 300 km to Site 534. The sediment likely did not travel that distance as an unconstrained sheet flow. However, if a submarine channel were available to "guide" the flow into the Basin, it would be able to flow much farther. Such a channel could occur on the deep-sea fan complex that has been seismically delineated by Sheridan et al. (1981), who have termed the thickest portion of it the Miocene Eleuthera Ridge (Fig. 13). The fan became extinct and later sediment was deposited over it; it is for the most part now a topographically buried ridge. However, south of Sites 391 and 534 there is a slight topographic high where this ancient fan complex is only partially buried (Fig. 15). This fan can be traced from near the confluence of Northwest and Northeast Providence Channels into the Blake-Bahama Basin, just west of Sites 391 and 534 (Fig. 14); we feel it aided or "guided" the debris flows this far into the Basin. Debris flows may constitute a large proportion of the sediment record near the mouth of Great Abaco Canyon and near the base of the Bahama platform, but they have not been cored.

The associated turbidites covered the Basin more easily. Indeed, they have been known to travel several hundred kilometers over slopes as low as 0.3° (Damuth and Embley, 1981; Elmore et al., 1978). The debris flows are mostly early Miocene, whereas the turbidites span the

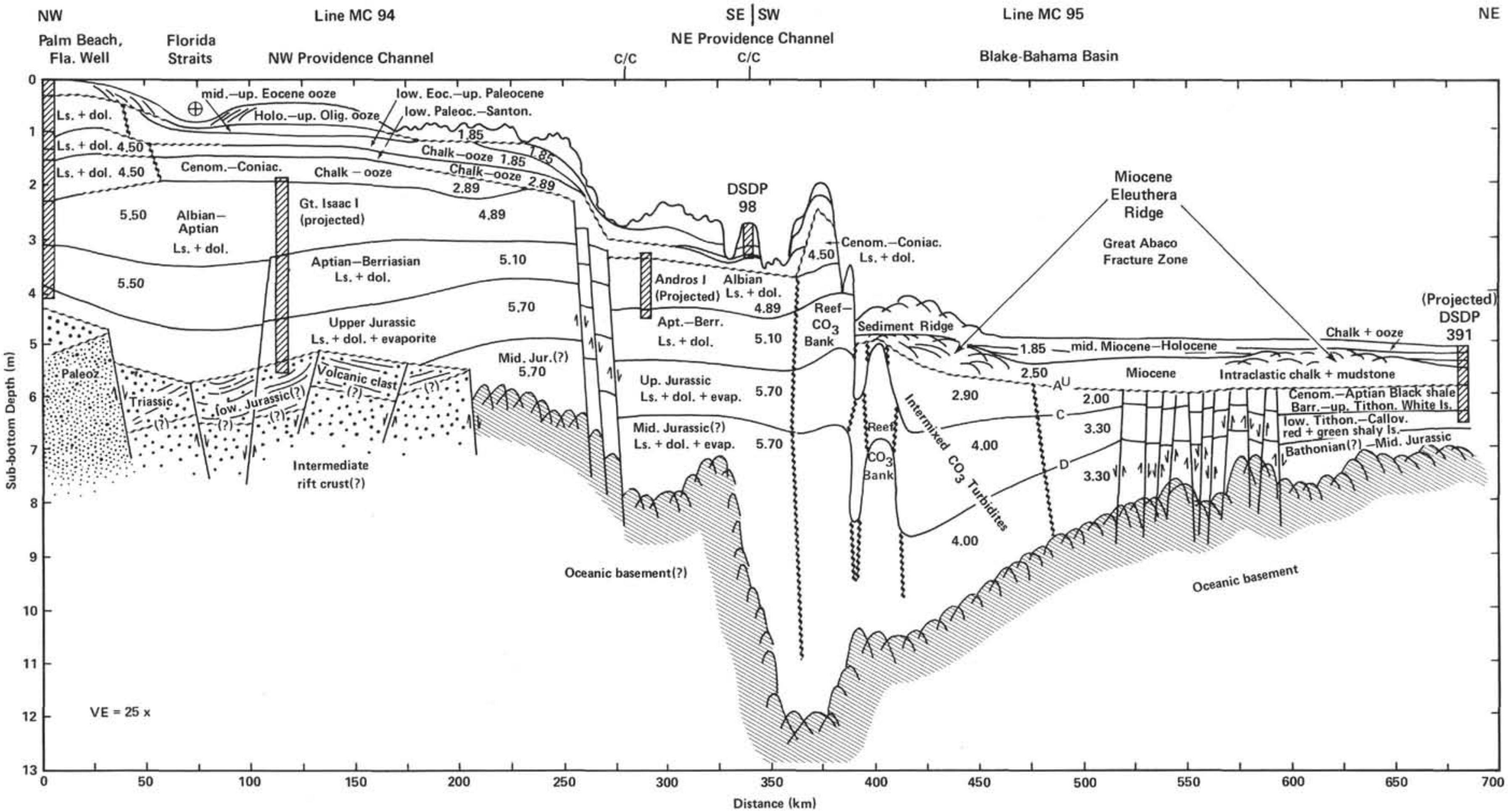

Figure 13. Structural cross-section through Northwest and Northeast Providence Channels and across the Bahama Escarpment to the Blake-Bahama Basin, based on depth conversion of lines MC 94 and MC 95. (Seismic interval velocities used for depth conversion are given in km/s. The location of the Miocene Eleuthera Ridge is indicated by the hummocky topography and hyperbolic reflectors created by the channels, levees, and microtopography of a deep-sea fan built by turbidites and debris flows [from Sheridan et al., 1981].)

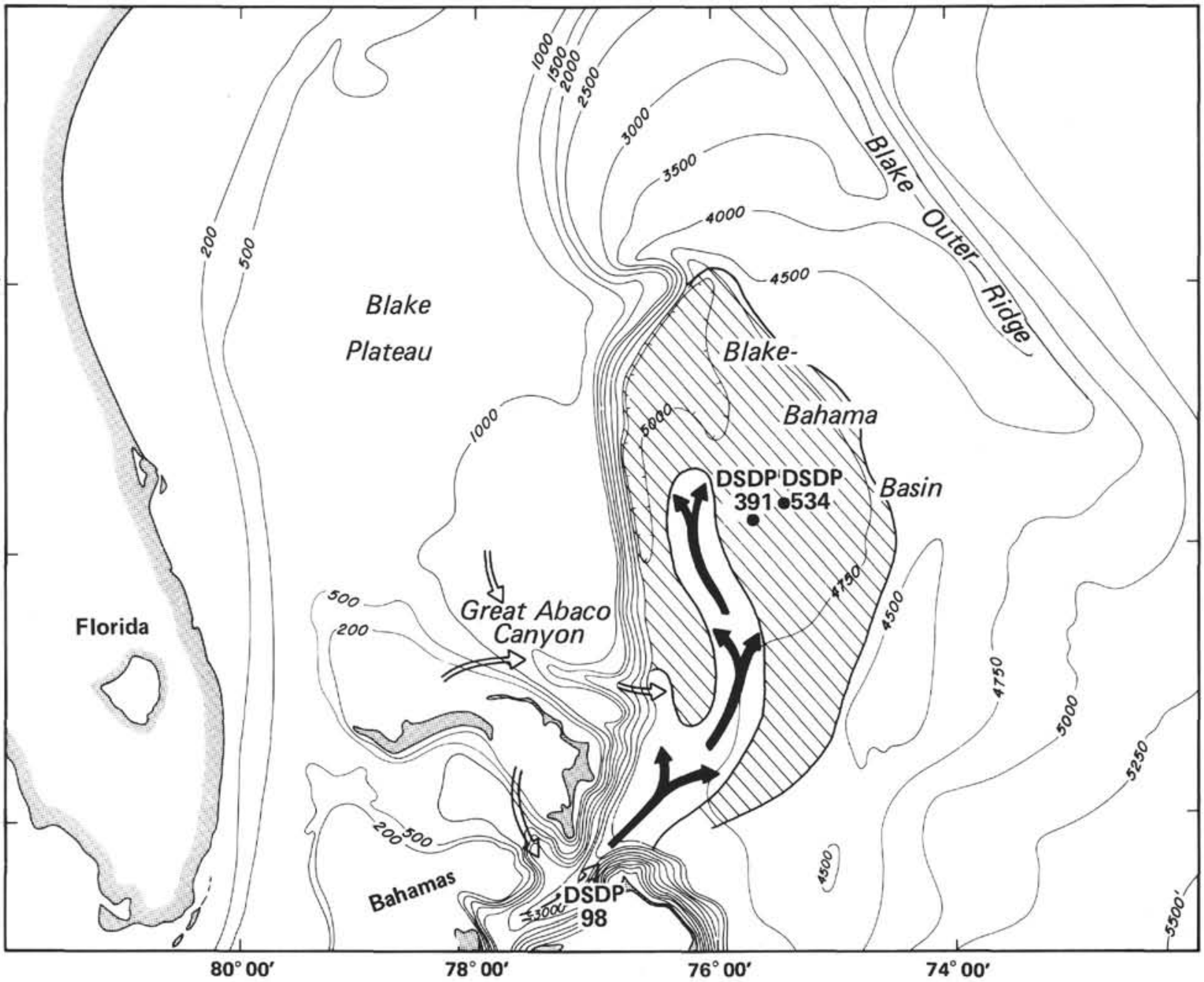

Figure 14. Map showing the interpreted depositional model for the Great Abaco Member. (Sources [indicated by open arrows] include the Blake Plateau and Escarpment, and the Bahama Banks, both platform and slope. The configuration of the Miocene Eleuthera Ridge just west of Sites 391 and 534 [white with solid arrows] indicates the path of sediment dispersal into the Blake-Bahama Basin by turbidite and debris-flow mechanisms. These deposits subsequently covered much of the Basin, and their present distribution is marked by the pattern of diagonal lines. Contours are in meters.)

whole Miocene (Fig. 13). The late Miocene turbidites, especially, are basin-levelling events. They can be mapped by reflector M (Fig. 15) and cover nearly all the present area of the Blake-Bahama Basin abyssal plain in a nearly horizontal blanket (Sheridan et al., 1974).

The turbidites and debris flows that floor the Blake-Bahama Basin were produced by catastropic slumping events, somewhat different than the more uniform growth of turbidite fans such as the Sohm and Hatteras fans to the north. These events punctuated the background sedimentation of siliceous mudstone, and gave rise to the distinctive and unusual appearance of the intraclastic chalks that characterize the Great Abaco Member. This sequence of lithologies is apparently unique to the western North Atlantic, as similar sequences have not been found off the coast of North Africa.

CONCLUSIONS

Detailed lithologic and biostratigraphic analysis of cores from the Blake-Bahama Basin has increased our knowledge and understanding of the provenance and deposition of distinctive intraclastic chalks found in the Miocene section. Five lithofacies were delineated and grouped into four subunits based on relative abundance of lithologic types. Siliceous mudstones are dominated by radiolarians, diatoms, and clay and comprise the background rain of pelagic sediments deposited below the carbonate compensation depth. Sedimentary structures indicate the mudstones may have been deposited, or at least reworked, by contour currents. The chalks are composed mainly of planktonic foraminifers and nannofossils, and the intraclastic facies also contains clasts of siliceous mudstone, chalk, and limestone. Some of the limestone clasts contain shallow-water foraminifers and are thus platform derived. Similarly the skeletal packstone facies contains both deep- and shallow-water constitutents and also reflects a mixed source. Composition of the debris-flow facies is similar to the packstones, with the large-scale sedimentary structures providing the main distinction.

Relationships between facies and sedimentary structures, such as scoured bases, grading, and clast align-

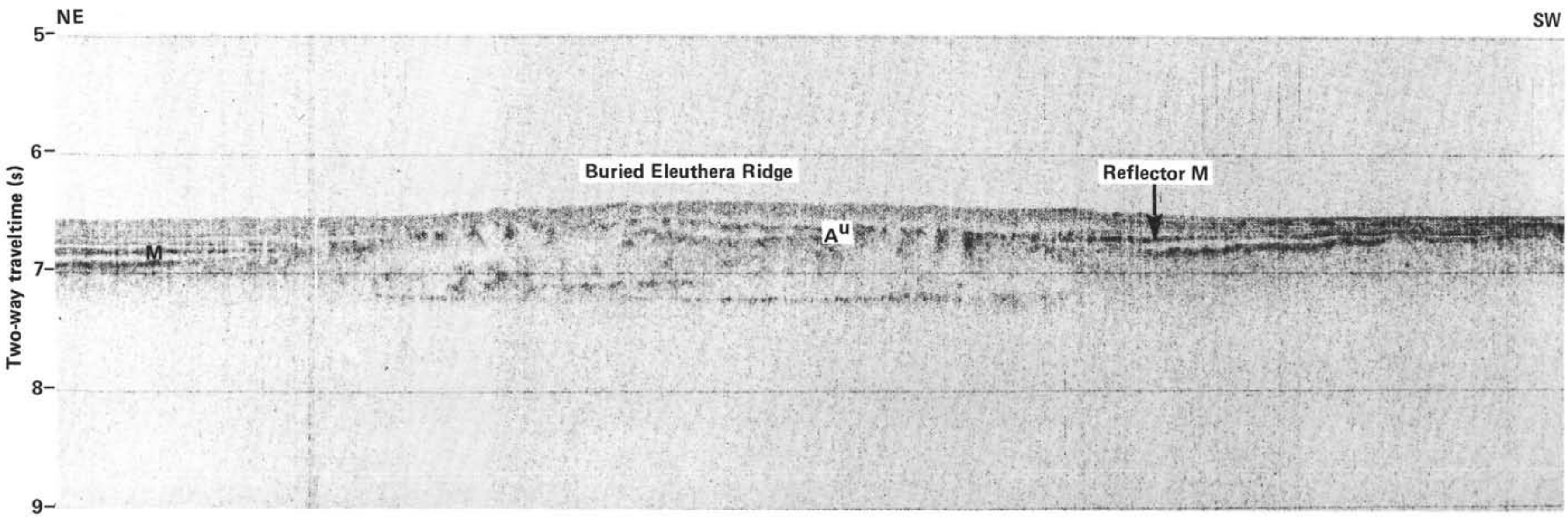

Figure 15. Photograph and interpretation of *Glomar Challenger* air-gun seismic reflection profile across the partially buried Eleuthera Ridge. (Note the turbidites and debris flows of reflector M spreading out from the Ridge.)

ment, indicate most of the facies were deposited by turbidity currents. However, clasts also float in the matrix and may be chaotically arranged, indicating debris-flow activity has also contributed to deposition of the sediment. These two mechanisms are part of a continuous spectrum and grade into one another over the sedimentary section recovered in this Basin. Although we have separated the sediment types resulting from these processes, perhaps the differentiation should not be so distinct.

The Great Abaco Member has not been exposed to fresh water or been buried very deeply and has consequently undergone little diagenesis. Compaction and cementation are the main types of alteration that have occurred. Micritic calcite is the dominant cement and has partially lithified the chalks. Occasionally, early generations of shallow-water cement can be seen in limestone clasts derived from platform margins and incorporated into the chalks.

All the carbonate material in the Great Abaco Member is redeposited and was derived from the Blake Plateau to the west and the Bahama Banks to the south. Deeper water foraminifer–nannofossil oozes from the Blake Plateau and Little Bahama Bank flowed out Great Abaco Canyon into the Blake-Bahama Basin as unconstrained, high-energy turbidites. Deeper-water material from more eastern slopes of the Bahamas flowed northward into the basin. Previously cemented limestones containing benthic foraminifers, red algae, and other shallow-water constituents were derived from shallow platform margins of the Bahama Banks and flowed northward into the Basin and also eastward through Great Abaco Canyon into the Basin. The triggering events probably include a combination of sea-level changes and earthquakes. Movement of wave base related to glacially induced sea-level changes plus sediment overloading would create sediment instability on platform margins. Tectonic activity along the Great Abaco Fracture Zone and faults in the northern Bahamas would induce large-scale failure of platform margin and slope sediments.

Constrained by channels in distributaries of a submarine fan (now called Eleuthera Ridge), the relatively coarse-grained debris flows traveled over 300 km across the Basin. The associated and subsequent turbidites traveled a similar distance, but more as unchanneled sheet flows. These turbidites cover the whole Basin and form the first prominant seismic reflector (M) in the Basin (Sheridan et al., 1974). Similar facies have not been found in corresponding localities in the eastern Atlantic. However, these deposits resemble some ancient, fine-grained turbidite debris-flow sequences and could be of use in reconstructing basin–platform relationships.

ACKNOWLEDGMENTS

We wish to thank Drs. S. F. Frost and G. A Seiglie of Gulf Exploration and Production Co. for identifications of algae and benthic foraminifers. P. M. Harris, Gulf Exploration and Production Co., read an early version of the manuscript and made many helpful suggestions. We thank H. T. Mullins, Moss Landing Marine Laboratories, and C. D. Crevello, Marathon Oil Company, for critically reviewing the manuscript.

REFERENCES

Benson, W. E., Sheridan, and Shipboard Scientific Party, 1978. Site 391: Blake-Bahama Basin. *In* Benson, W. E., Sheridan, R. E., et al., *Init. Repts. DSDP*, 44: Washington (U.S. Govt. Printing Office), 153–336.

Bouma, A. H., 1962. *Sedimentology of Some Flysh Deposits:* New York (Elsevier).

Bryan, G. M., Markl, R. G., and Sheridan, R. E., 1980. IPOD site surveys in the Blake-Bahama Basin. *Mar. Geol.*, 35:43–63.

Cook, H. E., McDaniel, P. N., Mountjoy, E. W., and Pray, L. C., 1972. Allochthonous carbonate debris flows at Devonian bank ("reef") margins, Alberta, Canada. *Bull. Can. Pet. Geol.*, 20: 439–497.

Crevello, P. D., and Schlager, W., 1980. Carbonate debris sheets and turbidites, Exuma Sound, Bahamas. *J. Sediment. Petrol.*, 50: 1121–1148.

Damuth, J. E., and Embley, R. W., 1981. Mass-transport processes on Amazon Cone: Western Equatorial Atlantic. *Am. Assoc. Pet. Geol. Bull.*, 65:629–643.

Elmore, R. D., Pilkey, O. H., Cleary, W. J., and Curran, H. A., 1979. Black shell turbidite, Hatteras Abyssal Plain, western North Atlantic. *Geol. Soc. Am. Bull.*, 90:1165–1176.

Enos, P., 1977. Flow regimes in debris flow. *Sedimentology*, 24: 133–142.

Ewing, J. I., Ewing, M., and Leyden, R., 1966. Seismic-profiler survey of the Blake Plateau. *Am. Assoc. Pet. Geol. Bull.*, 50: 1948–1971.

Ewing, M., Worzel, J. L., et al., 1969. *Init. Repts. DSDP*, 1: Washington (U.S. Govt. Printing Office).

Fisher, R. V., 1971. Features of coarse-grained, high-concentration fluids and their deposits. *J. Sediment. Petrol.*, 41:916–927.

Hampton, M. A., 1975. Competence of fine-grained debris flows. *J. Sediment. Petrol.*, 45:834–844.

________, 1972a. Transport of ocean sediments by debris flow. *Am. Assoc. Pet. Geol. Bull.*, 56:627. (Abstract)

________, 1972b. The role of subaqueous debris flow in generating turbidity currents. *J. Sediment. Petrol.*, 42:775–793.

Hayes, D. E., Frakes, L., and Shipboard Scientific Party, 1973. Leg 28 deep-sea drilling in the southern ocean. *Geotimes*, 18(6):19–24.

Heezen, B. C., Hollister, C. D., and Ruddiman, W. F., 1966. Shaping of the continental rise by deep geostrophic contour currents. *Science*, 152:502–508.

Hollister, C. D., and Heezen, B. C., 1971. Geological effects of ocean bottom currents, western North Atlantic. *In* Gordon, A. L. (Ed.), *Studies in Physical Oceanography* (Vol. 2): New York (Gordon & Breach), 37–66.

Jansa, L. F., Enos, P., Tucholke, B. E., Gradstein, F. M., and Sheridan, R. E., 1979. Mesozoic-Cenozoic sedimentary formations of the North American Basin, western North Atlantic. *In* Talwani, M., Hay, W., and Ryan, W. B. F. (Eds.), *Deep Drilling Results in the Atlantic Ocean: Continental Margins and Paleoenvironments:* Am Geophys. Union, Maurice Ewing Series, 3:1–57.

JOIDES (Joint Oceanographic Institutions' Deep Earth Sampling Program), 1965. Ocean drilling on the Continental margin. *Science*, 50:709–716.

McIlreath, J. A. and James, N. P., 1979. Carbonate slopes. *In* Walker, R. G., (Ed.), *Facies Models.* Geoscience Canada Reprint Series, 1:133–143.

Maher, J. C., 1965. Correlations of Mesozoic and Cenozoic rocks along the Atlantic coast. *Am. Assoc. Pet. Geol.*, Cross Section 3.

Middleton, G. V., and Hampton, M. A., 1973. Sediment gravity flows: Mechanics of flow and deposition. *Turbidites and Deep-Water Sedimentation.* Soc. Econ. Paleontol. Mineral. Pacific Sect., Short Course, pp. 1–38.

Mountjoy, E. W., Cook, H. E., Pray, L. C., and McDaniel, P. M., 1972. Allochthonous carbonate debris flows–worldwide indicators of reef complexes, banks or shelf margins. *Int. Geol. Cong. 24th Proc. Sect.*, 6:172–189.

Mullins, H. T., Keller, G. H., Kofoed, J. W., Lambert, D. N., Stubblefield, W. L., and Warme, J. E., in press. Geology of Great Abaco Submarine Canyon: observations from the research submersible "ALVIN". *Mar. Geol.*

Mullins, H. T., and Van Buren, H. M., in press. Walkers Cay Fault, Bahamas: evidence for Cenozoic faulting. *Geo-Marine Lett.*

Paulus, F. J., 1972. The geology of Site 98 and the Bahama Platform. *In* Hollister, C. D., Ewing, J. I., et al., *Init. Repts. DSDP*, 11: Washington (U.S. Govt. Printing Office), 877–897.

Shanmugam, G., 1980. Rhythms in deep sea, fine-grained turbidite and debris-flow sequences, Middle Ordovician, eastern Tennessee. *Sedimentology*, 27:419–432.

Shanmugam, G., and Benedict, G. L., III, 1978. Fine-grained carbonate debris flow, Ordovician basin margin, southern Appalachians. *J. Sediment. Petrol.*, 48:1233–1240.

Sheridan, R. E., 1974. Atlantic margin of North America. *In* Burk, C. A., and Drake, C. L. (Eds.), *The Geology of Continental Margins:* New York (Springer-Verlag), pp. 391–407.

Sheridan, R. E., Berman, R. M., and Corman, D. B., 1971. Faulted limestone block dredged from Blake Escarpment. *Geol. Soc. Am. Bull.,* 82:199–206.

Sheridan, R. E., Crosby, J. T., Bryan, G. M., and Stoffa, P. L., 1981. Stratigraphy and structure of Southern Blake Plateau, Northern Florida Straits and Northern Bahama Platform from multichannel seismic reflection data. *Am. Assoc. Pet. Geol. Bull.*, 65: 2571–2593.

Sheridan, R. E., Golovchenko, X., and Ewing, J. I., 1974. Late Miocene turbidite horizon in Blake-Bahama Basin. *Am. Assoc. Pet. Geol. Bull.*, 58:1797–1805.

Sheridan, R. E., and Osburn, W. L., 1975. Marine geologic and geophysical studies of the Florida-Blake Plateau-Bahamas area. *Can. Soc. Pet. Geol. Mem.,* 9:9–32.

Tator, B. A., and Hatfield, L. E., 1975. Bahamas present complex geology. *Oil Gas J.* , 73(43):172–176 and 73(44):120–122.

Walker, R. G., 1979. Turbidites and associated coarse clastic deposits. *In* Walker, R. G. (Ed.), *Facies Models:* Geoscience Canada Reprint Series, 1:91–103.

Date of Initial Receipt: April 21, 1982